

AD _____

Award Number: DAMD17-99-1-9073

TITLE: Research Training Program in Breast Cancer

PRINCIPAL INVESTIGATOR: Daniel Medina, Ph.D.

CONTRACTING ORGANIZATION: Baylor College of Medicine
Houston, Texas 77030

REPORT DATE: July 2003

TYPE OF REPORT: Annual Summary

PREPARED FOR: U.S. Army Medical Research and Materiel Command
Fort Detrick, Maryland 21702-5012

DISTRIBUTION STATEMENT: Approved for Public Release;
Distribution Unlimited

The views, opinions and/or findings contained in this report are those of the author(s) and should not be construed as an official Department of the Army position, policy or decision unless so designated by other documentation.

20040226 089

REPORT DOCUMENTATION PAGEForm Approved
OMB No. 074-0188

Public reporting burden for this collection of information is estimated to average 1 hour per response, including the time for reviewing instructions, searching existing data sources, gathering and maintaining the data needed, and completing and reviewing this collection of information. Send comments regarding this burden estimate or any other aspect of this collection of information, including suggestions for reducing this burden to Washington Headquarters Services, Directorate for Information Operations and Reports, 1215 Jefferson Davis Highway, Suite 1204, Arlington, VA 22202-4302, and to the Office of Management and Budget, Paperwork Reduction Project (0704-0188), Washington, DC 20503

1. AGENCY USE ONLY (Leave blank)		2. REPORT DATE July 2003	3. REPORT TYPE AND DATES COVERED Annual Summary (1 Jul 2002 - 30 Jun 2003)	
4. TITLE AND SUBTITLE Research Training Program in Breast Cancer			5. FUNDING NUMBERS DAMD17-99-1-9073	
6. AUTHOR(S) Daniel Medina, Ph.D.				
7. PERFORMING ORGANIZATION NAME(S) AND ADDRESS(ES) Baylor College of Medicine Houston, Texas 77030 <i>E-Mail:</i> dmedina@bcm.tmc.edu			8. PERFORMING ORGANIZATION REPORT NUMBER	
9. SPONSORING / MONITORING AGENCY NAME(S) AND ADDRESS(ES) U.S. Army Medical Research and Materiel Command Fort Detrick, Maryland 21702-5012			10. SPONSORING / MONITORING AGENCY REPORT NUMBER	
11. SUPPLEMENTARY NOTES				
12a. DISTRIBUTION / AVAILABILITY STATEMENT Approved for Public Release; Distribution Unlimited				12b. DISTRIBUTION CODE
13. ABSTRACT (Maximum 200 Words) The goal of this research training program is to produce highly qualified scientists for careers as independent investigators in the field of breast cancer. During the last 25 years, there has been a fundamental revolution in the understanding of molecular and cell biological concepts related to cell growth, function and tumorigenesis. To utilize what has been learned and to continue future progress in the area of breast cancer requires the continued availability of well-trained, innovative and committed scientists. This program represents an interdepartmental training program involving 15 investigators from seven departments. Trainees are predoctoral and postdoctoral fellows with backgrounds in biochemistry, cell and molecular biology, molecular genetics and molecular virology. The training program provided trainees with additional foundation in carcinogenesis and breast cancer. In addition to the core curriculum taken by the predoctoral fellow in their respective academic departments, program enhancement is provided through trainees' participation in a graduate course on "Molecular Carcinogenesis" (predoctoral fellows), a Breast Disease Research Seminar (all trainees) and participation at national meetings and local seminars. Predoctoral and postdoctoral trainees are enrolled in the program.				
14. SUBJECT TERMS Breast cancer				15. NUMBER OF PAGES 37
				16. PRICE CODE
17. SECURITY CLASSIFICATION OF REPORT Unclassified	18. SECURITY CLASSIFICATION OF THIS PAGE Unclassified	19. SECURITY CLASSIFICATION OF ABSTRACT Unclassified	20. LIMITATION OF ABSTRACT Unlimited	

Table of Contents

Cover.....	1
SF 298.....	2
Table of Contents.....	3
Introduction.....	4
Body.....	5-12
Key Research Accomplishments.....	11
Reportable Outcomes.....	11-12
Conclusions.....	12
References.....	N/A
Appendices.....	13-37

INTRODUCTION

Breast cancer is a complex disease whose ultimate understanding will require the integration of facts resulting from a multidisciplinary approach. Continued basic science research will provide a fuller understanding of the basic mechanisms of breast cancer that is necessary to conquer the disease in humans. In order to have the scientific human armamentarium to further this understanding, this training grant focuses on producing qualified scientists for careers as independent investigators in the area of breast cancer. The rationale for a targeted training grant in breast cancer is based on the belief that the elucidation of how oncogenes, tumor suppressor genes, hormones and growth factors act at the molecular level and as developmental-specific agents are critical questions directly relevant to the etiology, prevention, diagnosis, treatment and prognosis of human breast cancer. The training program has drawn together individuals who have an established research and training background in the mammary gland with individuals who have a research and training background in cell biology, molecular endocrinology, molecular biology, molecular virology, viral oncology, molecular genetics and biochemistry. The strength of the program is two-fold. First, the program gathers together members of diverse disciplines to focus on the training of predoctoral and postdoctoral students for careers in an area that, by its biological nature, is multi-disciplinary. Second, the program introduces new intellectual approaches and insights to the problem of breast cancer that will be continued by the next generation of research scientists.

The design of the training program provides for trainees to be exposed to clinical problems and recent advances as well as the multi-disciplinary approaches to answering fundamental questions related to breast cancer research. The familiarity and close proximity of the training faculty facilitates and encourages the development of a new generation of research scientists who will be able to understand the problem of breast cancer at a more complex level and from a multi-disciplinary orientation.

BODYa. Trainees

The goal of this training program is to provide an environment for training in breast cancer research. To foster this goal, candidate graduate students have to meet a minimum set of requirements. Graduate students have to be at least in their second year of graduate school and have selected a thesis problem focusing on an aspect of mammary gland growth, differentiation and/or cancer. These students are supported for two years by the training program provided they maintain satisfactory progress in their research program and they participate in the weekly "Breast" seminar and attend the course "Molecular Carcinogenesis". The postdoctoral fellows are supported by the training program for two to three years provided they maintain satisfactory progress in their research project and actively participate in the weekly "Breast" seminar. The six fellows from the grant year 2002 - 2003, their departmental affiliation, mentor, research problem and an Abstract of their research is provided below.

b. Research Projects

- 1) Geetika Chakravarty, Ph.D., Department of Molecular and Cellular Biology; Mentor, Jeffrey Rosen, Ph.D., Professor; "p190-B in mammary development and cancer."

The overall objective of this fellowship was to establish that p190-B expression is critical for ductal morphogenesis and that its aberrant expression facilitates cancer progression. Functional studies of p190-B that are being pursued to address these objectives are described in the following section.

RhoGAP-p190-B is essential for mammary development: Since p190-B null mice are perinatal lethal, the property of the mammary epithelium to regenerate following transplantation into the cleared fat pad, was utilized to determine how p190-B might contribute to embryonic and virgin mammary gland development. Interestingly, loss of both alleles of p190-B resulted in a complete failure of outgrowth of the transplanted mammary anlage, and approximately a 50% decrease in the take rate for the heterozygous embryos. In addition, a statistically significant decrease in the rate of ductal outgrowth(s) as compared to wildtype mice was observed for p190-B heterozygotes at four and five weeks of age. This appears to result from decreased proliferation in the cap cells of the TEBs and was quite similar to the decreased proliferation observed previously in the cap cells of TEBs from outgrowths derived from the IGIR null mice.

p190-B-null mammary buds fail to grow out as a result of perturbed epithelial-mesenchymal interactions. Retarded embryonic mammary development as a result of improper epithelial-mesenchymal interactions was detected in the p190-B null embryos and to a lesser extent in the heterozygotes as determined using tenascin C as a marker for the mesenchyme, and p63 as a marker of the epithelium, respectively. These studies indicated that the size of the mammary bud was decreased in the p190-B null embryos and that the mesenchyme surrounding the bud was disorganized. In addition, preliminary in situ hybridization studies suggest that p190-B may be preferentially expressed in the epithelial bud and that loss of p190-B may result in decreased migration and increased apoptosis of the epithelial cells in the mammary bud, as

well as a disruption of inductive signals to the mesenchyme required. Additional analysis of the mammary anlage from day E10 to E15 are in progress.

Generation of TetOp190-B mice and Dox regulated p190-B MCF-7 cell clones.

To study the mechanism by which p190-B overexpression might regulate cell migration and responsiveness to estrogen and IGF-I as well as breast cancer progression, we wanted to generate both stable cell lines and transgenic mouse models. Preliminary attempts to generate stable cell lines expressing p190-B indicated that use of a regulatable system would be preferable to be able to directly relate the phenotype observed in stable cell clones to the levels of p190-B expression. A few stable clones expressing p190-B were generated using MCF10AT normal breast cells and MDA-435 breast cancer cell lines. The preliminary examination of these clones indicated that the p190-B expressing clones exhibited a complete loss of the actin stress fibers, as well as the loss of well defined cell-cell junctions. In addition they were less adherent and therefore potentially more invasive. Consistent with these latter findings, the induction of the matrix metalloprotease, MMP-2 was detected in cells overexpressing p190-B. Thus, we decided to generate both Tet-regulatable transgenic bigenic mice and MCF-7 cell lines.

To generate a Tet inducible p190-B transgenic mice, the following reporter construct was generated. The p190-B cDNA was subcloned into the EcoRI site of PUHD10-3 plasmid (a gift from Dr. Bujard) downstream of a CMV minimal promotor and seven adjacent Tet operator sites derived from pTet-Splice. SV40 splicing and polyadenylation signal sequences were downstream of the p190-B cDNA. Restriction fragments containing the entire transgene were isolated from vector sequences and purified for microinjection into fertilized oocytes of FVB/N mice. Before injecting the DNA, the transgene construct was tested for inducibility *in vitro* by transiently transfecting it into tTA expressing MCF-7 cells. The transgene was readily induced by adding 2 mg/ml doxycycline to the medium after 12 – 24 hrs of transfection. The same transgene has been also stably transfected into tTA expressing MCF-7 cells. Efforts are underway to select several tightly regulated clones.

Four founder mice from a single round of injection have been generated. To test the inducibility of the transgene, these lines are currently being bred to generate bigenic mice. To facilitate these studies, the MMTV-rTA-pA (MTB) line expressing the reverse tetracycline transactivator was kindly provided by Dr. Lewis Chodosh at the University of Pennsylvania. Currently, the Tetop190-B mice are being crossed to these MTB line to ascertain the inducibility of the transgene *in vivo*.

- 2) Li-Ru You, Ph.D., Department of Molecular and Cellular Biology; Mentor, Sophia Tsai, Ph.D., Professor; "Role of COUP-TFII in mammary gland development and tumorigenesis."

COUP-TFII is a member of orphan nuclear receptor superfamily. The expression pattern of *COUP-TFII* suggests that it participates in mesenchymal-epithelial interactions required for organogenesis. The null mutants of *COUP-TFII* die around embryonic day 10 with angiogenesis and heart formation defect, while two-thirds of heterozygotes die before weaning. To further understanding the biological functions of *COUP-TFII* during development, the mouse with floxed *COUP-TFII* allele was generated.

To elucidate the function of *COUP-TFII* in mesenchymal-epithelial interactions, mammary gland is a classic example for this purpose. Both formation of mammary bud and ductal branching morphogenesis are critically dependent on a series of reciprocal and sequential signals exchanged between the mammary mesenchyme and mammary epithelium. Our preliminary result shows that, during embryonic mammary bud development, COUP-TFII is

initially expressed in both mammary epithelium and mammary mesenchyme. At embryonic day 18, *COUP-TFII* expression in epithelium ceases, while its expression in surrounding mesenchyme remains the same. The critical period for changes of *COUP-TFII* expression patterns and the physiological functions during mammary bud formation were further investigated. After birth, *COUP-TFII* is expressed in stromal cells. Mammary gland whole mounts and morphometric analysis show that ductal growth in *COUP-TFII* heterozygous virgin appears somewhat faster than mammary gland of aged matched wild type littermate, suggesting potential changes in hormone responses. Mammary glands of the male mice have also been examined. Our preliminary result shows that at least 60% of *COUP-TFII* heterozygous males still have ductal glands. Some of glands in these male mice reach the stroma around lymph node area. In contrast, aged matched wild type littermates either do not possess glands or only remnants of glands remain. In the male mice, the effects of androgen-mediated apoptosis in the mammary epithelium lead to the regression of the gland at E14.5. The abnormal mammary gland development in the *COUP-TFII* heterozygotes indicates that *COUP-TFII* is important for mammary development. To further address this question, the hormonal levels and its mediated effects in both female and male *COUP-TFII* heterozygous mice are currently under investigation.

The early embryonic lethality of *COUP-TFII* null mutant and the lack of stromal cell specific Cre mouse render it difficult to determine the functions of *COUP-TFII* in mammary development. However, in addition to mesenchymal-epithelia interactions, vasculature in the gland also contributes to mammary gland development. Using endothelial cell-lineage specific Tie2-Cre to disrupt the expression of *COUP-TFII* will enable us to examine the function of *COUP-TFII* in vasculature formation in mammary gland morphogenesis. We have successfully generated Tie2-Cre endothelial specific *COUP-TFII* knockout mice and these conditional *COUP-TFII* null mice die at E12 with severe hemorrhage. This result suggests that the endothelial expression of *COUP-TFII* is essential for embryonic survival.

- 3) Y. David Lee, Department of Biochemistry; Mentor, Stephen Elledge, Ph.D., Professor; "Mechanistic dissection of *mec1* in replicational stress."

To ensure the genetic code is passed down to daughter cells with high fidelity, pathways have evolved to arrest cell cycle, repair damage, and alleviate the condition when cells encounter endogenous or exogenous genotoxic stress. Hydroxyurea (HU) induces one such type of stress (replicational) by inhibiting subunit of ribonucleotide reductase complex (Rnr2), depleting the dNTP pools and stalls replication forks during DNA synthesis. In *Saccharomyces cerevisiae*, stalled replication forks is sensed, transduced, and eventually results in fork stabilization, inhibition of firing of late origin of replication, spindle arrest, transcriptional activation of all RNR subunits, degradation of RNR inhibitor Sml1, and translocation of Rnr2/4 subunit from the nucleus to the cytoplasm to form active RNR complex. The combined effects help to arrest cell cycle, prevent additional forks from collapsing, and increase dNTP production. *MEC1* and *RAD53* are both kinases important in the transduction step. *mec1Δ* and *rad53Δ* are both lethal. This lethality, but not HU sensitivity (HU^S), can be suppressed by various mechanisms that increase dNTP pools, such as the deletion of *SML1* (a negative regulator of RNR complex).

The first project was designed to look for suppressors of *mec1*'s HU^S, which can yield additional information on how cells respond to replicational stress. A CEN *URA GAL1::cDNA* over-expression library was transformed into *mec1Δ sml1Δ* background to look for colonies that can now grow on 20mM HU. One gene WTM2 (WD40-containing

transcriptional modulator 2) appeared many times as different cDNA species. Wtm2 and its homologue Wtm1 are nuclear proteins and are found to interact with each other. According to the BIND molecular-interaction database, over-produced Wtm2 can bind to Rnr2 and Rnr4, suggesting that the HU^R mechanism may be post-translational. I first verified that endogenous Wtm2 also binds to Rnr2/4 by Co-IP, and then showed that over-producing Wtm2 leads to an increase in the abundance of Rnr2 and Rnr4. Over-producing Wtm2 does not activate a *RNR3::reporter* construct, suggesting that the mechanism of HU^R is probably not due to a global transcriptional activation of the DNA-damage checkpoint. And even though *wtm2Δ* have no observable phenotypes, *wtm1Δ* in *mec1Δ sml1Δ* background was found to be five times more resistant at certain dosage of UV and HU. In addition, Rnr2 and Rnr4, which are usually present in the nucleus except during S-phase, lost their nuclear localization in *wtm1Δ* single mutant. The same observation is made in the absence of functional *MEC1*, *RAD53*, and *DUN1*, and is also cell-cycle independent. Given the above data, it is likely that Wtm1 and Wtm2 are important regulators of Rnr2/4's localization, possibly playing a role in anchoring or transporting Rnr2/4. Because the localization of Rnr2/4 is affected by cell cycle and genotoxic agents such as HU and MMS, it is also possible that a checkpoint may affect the localization of Rnr2/4 via the Wtm proteins. Since Wtm1 and Wtm2 each has 4 and 5 SQ sites, respectively (which may be phosphorylated in response to replication stress or DNA-damage), I am currently testing for any changes in the abundance or post-translational modification after HU-treatment. It also remains to be tested whether Wtm1 also binds to Rnr2/4 like Wtm2, and if there is any functional significance of binding to Rnr2/4, or if this binding is affected by cell-cycle progression, HU, or other forms of DNA-damage.

The second project involves 123 HU^S-mutants which showed greater lost of viability in 200mM HU compare to wildtype, isolated by former members of this lab. 53/123 of these mutants were identified to single loci. The goal of this project is to identify the rest of the mutants whose HU^S is rescued by *RAD53* over-production, possibly yield more components of the *MEC1/RAD53* pathway. So far, all 123 mutants have been transformed by a *RAD53* over-expression vector, and each transformant as well as their respective parental strains have been tested for growth on minimal level of HU. For those transformants that showed greater growth on particular HU concentration compare to the parental mutant strain, complementation analysis will be done and genes identified.

- 4) Charalambos (Harry) Toumazou, Department of Molecular and Cellular Biology; Mentor, Adrian Lee, Ph.D., Assistant Professor; Breast Center, "Cross-talk between ER and IGF in human breast cancer."

The first project involved the use of the MCF10AT cell line. This is a transformed human cell line that forms ductal structures when grown on an extracellular matrix. MCF10AT were derived from MCF10A an immortalized normal cell line with no Estrogen Receptor (ER) expression. Unlike their parental cell line MCF10AT have been shown to express ER. Their ER status and their growth properties made this cell line an ideal model for the study the crosstalk between the ER and IRS pathways. Before the experiments started I wanted to see if the ER pathway was restored in these cells as stated by a publication. Despite loading very high amounts of total protein we were unable to visualize the protein through western blot analysis. To explore the possibility that the protein is expressed at levels that are below the detection limit of our antibodies we performed two other types of experiments, cell proliferation and DNA binding/transcriptional activation assays. The capacity for cell proliferation and the control of cell proliferation by ER was analyzed by flow cytometry and growth curves. The

results from both these assays showed that estrogen (E_2) administration had absolutely no effect on the rate of cell proliferation. This lack of response to E_2 is in agreement with the results from the western blots in suggesting that MCF10AT do not express ER. However, upon careful reviewing of the flow cytometry data, we decided that the issue of media selection and the impact that may have on the results, needs to be resolved before any conclusions are reached. The ERE-luciferase plasmid, which contains the Estrogen Response Element upstream of the luciferase gene, was transiently transfected in MCF7 and MCF10AT cells. Transcriptional activation by ER binding to and activating the ERE is measured through the expression of luciferase. The results from these assays verify that under the experimental conditions used, MCF10AT cells have no functional endogenous ER.

The second project involved the generation of cell lines that express compartment specific variants of ER. Stable clones that express exclusively cytoplasmic ER (cER) conjugated to GFP have been successfully generated. The generation of a membrane specific variant of ER proves more elusive than the cytoplasmic form. Previous attempt to target ER to the membrane using a prenylation tag show failed to show the correct localization. To generate the membrane variant, I have chosen to use a myristylation tag attached to the N terminus of the protein. I believe that this will enable the proper folding of the protein and allow the desired sub-cellular localization. This project is ongoing.

- 5) Bonnie W. Nannenga-Combs, Department of Molecular Virology and Microbiology; Mentor, Larry Donehower, Ph.D., Professor; "Role of Wip1 in mammary tumorigenesis."

Wip1 (Wildtype p53 Induced Phosphatase/PPM1D) is amplified and overexpressed in 11-16% of human breast cancers. Additionally, gain of the amplicon containing Wip1 has been associated with neuroblastomas and poor prognosis in Ovarian Clear Cell Adenocarcinomas. To study the oncogenic functions of Wip1, I created a series of mWip1 mutants. These mutants include six truncation mutants obtained through PCR. In addition, I have used site-directed mutagenesis to create point mutants that alter critical amino acids in the conserved phosphatase region. The mutants will be used in phosphatase and transformation assays. I hope to determine if the phosphatase activity of Wip1 is required for its transforming phenotype. As an *in vivo* model for Wip1's possible role in mammary tumor formation I have designed and injected an MMTV-mWip1 cDNA construct. I have identified four transgene positive founders using a transgene specific PCR genotyping strategy. I am currently monitoring these lines for tumors, assaying Wip1 expression, and screening for possible morphological and histological differences in mammary structure. Additionally, I will look for changes in tumor susceptibility compared to wild-type following DMBA treatment.

Our lab has developed a Wip1 knockout mouse. These mice contain a deletion of Wip1 exons 4 and 5. Functional Wip1 protein is not made, providing a resource for studying the critical functions of Wip1. Work has been done to characterize the Wip1 null mice and the mouse embryonic fibroblast (MEF) lines derived from these animals. Interestingly, male null mice show reduced growth, fertility and viability. There is evidence of reduced immune function in the null mice as indicated by compromised function of both B and T cells, as well as significantly reduced resistance to immune challenge. Using flow cytometry we have found that Wip1 null cells accumulate at the G2/M checkpoint. This data supports mediation of p53 regulation by Wip1 at certain points in the cell cycle. Further, it has been shown that the phosphorylation status of p53 and expression of p53 down stream targets are indirectly

influenced by Wip1 expression. Recently, our lab has identified two novel Wip1 interacting proteins, UDG (Uracil DNA Glycosylase) and delta Polymerase. UDG and delta Polymerase are involved in Base Excision Repair (BER). We have found that Wip1 suppresses UDG mediated BER activity.

I have been monitoring wip1-nullxMMTV-wnt crosses for mammary tumors. Data collection for this study includes noting time of tumor formation, formalin fixation and freezing of tumor samples at time of harvest. Although these animals do not appear to have altered tumor latency, in collaboration with Albert Fornace, Ph.D. (NCI) we have seen a delay in tumors in wip1-nullxMMTV-c-neu and wip1-nullxMMTV-v-Ha-ras. We are continuing collaborations with Daniel Medina, Ph.D. (BCM) to look at Wip1 null mice as a potential model for increased p53 activity, specifically as a protection against mammary tumors. Interestingly, the Wip1 null mice exposed to DMBA have not survived treatment in contrast to their wildtype littermates. We are currently testing these mice for clues regarding the elevated sensitivity to DMBA. Results of these tests are pending. Wip1 knockout mice are also being crossed with p53 null mice. With the mice generated from these crosses we hope to gain a better understanding of the p53 dependent and independent functions of mWip1.

6) Isabel Latorre, Department of Molecular Virology and Microbiology; Mentor, Ron Javier, PH.D., Associate Professor; "Examining roles for *MUPP1*, *MAGI-1*, *ZO-2* and *DLF* in Mammary Carcinogenesis."

Human adenovirus type 9 generates mammary tumors in rats, and the primary oncogenic determinant of this virus is its E4-ORF1 oncoprotein. Our lab has shown that a PDZ domain-binding motif at the carboxyl-terminus of E4-ORF1 is required for it to interact with a select group of cellular PDZ-proteins, including MUPP1, MAGI-1, ZO-2 and DLG, to stimulate the phosphatidylinositol 3-kinase (PI3K) pathway, and to promote mammary tumors. Additionally, several lines of evidence suggest that the PDZ protein targets of E4-ORF1 may be tumor suppressors. Therefore, the aims of my project are to determine whether one or more of the E4-ORF1-associated PDZ proteins functions as a tumor suppressor and supports E4-ORF1-mediated PI3K activation.

In one set of experiments, I have targeted PDZ-protein genes for disruption in mice in order to determine whether the mutant animals display an increased incidence of tumorigenesis. *MAGI-1*^{-/-} mice are indistinguishable from their wild-type littermates at 11 months of age. We continue to age these mutant mice in an attempt to reveal an increased susceptibility to cancer. *ZO-2* mice. To date, I have been unable to obtain viable *ZO-2*^{-/-} mice (out of 31 mice screened), suggesting that *ZO-2* may be required for embryonic development. I am currently attempting to determine the embryonic stage at which lethality may occur. *MUPP1* mice. I have succeeded in isolating an embryonic stem cell clone with one *MUPP1* allele disrupted.

In a second set of experiments, I have examined the possible roles for individual PDZ proteins in PI3K activation by E4-ORF1. Preliminary results reveal that E4-ORF1 activates PI3K similarly in mouse embryo fibroblasts (MEF) derived from wild-type mice, *MAGI-1*^{-/-} mice, and *MUPP1*^{-/-} mice. These results suggest that neither MAGI-1 nor MUPP1 is essential for E4-ORF1-induced PI3K activation. However, E4-ORF1-induced PI3K activation is substantially reduced in *DLG*^{-/-} MEF compared to *DLG*^{+/+} MEF, suggesting that DLG is important for E4-ORF1-induced PI3K activation. This defect of *DLG*^{-/-} MEF is specific because these cells show normal PI3K activation following stimulation by growth factors. More important, over-expression of wild-type DLG splicing variants I3 and I1/I3, but not I2 or I1/I2, in

DLG^{-/-} MEF specifically enhances E4-ORF1-induced PI3K activation, suggesting that I3-containing isoforms specifically contribute to this activity.

In summary, I have found that MAGI-1 is dispensable for normal mouse development, whereas ZO-2 appears to be required. Additionally, I have shown that while MAGI-1 and MUPP1 are dispensable for E4-ORF1-induced PI3K activation, I3-containing DLG isoforms are important for this activity. Because E4-ORF1 promotes exclusively mammary tumors, I expect that these studies will reveal exciting unexpected roles for the E4-ORF1-associated PDZ proteins in mammary cell growth, development, and neoplasia.

KEY RESEARCH ACCOMPLISHMENTS

The major results of the past year in bullet form are:

- P190-B, a RhoGTPase, regulates mammary ductal morphogenesis.
- The transforming potential of the adenovirus E4-ORF1 oncoprotein functions through activation of P13K through a novel PDZ protein.
- Two novel Wip1 interacting proteins have been identified, uracil DNA Glycosylase and delta Polymerase. Wip1 suppresses UDG-mediated BER activity.

REPORTABLE OUTCOMES

Enhancement Programs

Three education programs specific for this training program were functional over the past year. The bi-weekly "Breast" seminar included faculty and trainees. The schedule for the seminar series is shown in Table 1.

The second education enhancement program is the Invited Speakers program. This program allows both the faculty and fellows supported by the program to interact with the invited speaker. The speakers were Dr. Max Wicha (University of Michigan Cancer Center) on "Mammary stem cells," Dr. Jeffrey Pollard (Albert Einstein College of Medicine) on "Immune cell regulation of mammary growth, and Dr. Lewis Chodosh (University of Pennsylvania School of Medicine) on "New genetically engineered mouse models to study mammary development and cancer."

The third education enhancement program is the course in "Molecular Carcinogenesis," which is given every Winter bloc and each predoctoral trainee is required to pass. This course is organized by Dr. Larry Donehower and the teaching faculty includes Drs. Medina, Harper, Donehower and Brown.

Trainee Review

With respect to trainee review, five of the six trainees continue in their research programs. Dr. Geetika Chakraverty finished her postdoctoral tenure and is now a Research Instructor in the Department of Molecular and Cellular Oncology, M.D. Anderson Cancer Center, Houston, Texas.

The training grant has finished its eighth year. Unfortunately, USAMRC has not continued this highly valued research training program (Institutional Training Grants) in their portfolio.. Our grant has received a no-cost extension for one year and Bonnie Nannenga, a predoctoral fellow, will continue her research and be supported by remaining funds in our grant.

Publications

Two of the supported trainees have publications in leading scientific journals. These are listed below and are provided as appendices.

1. Chakravarty, G., Hadsell, D., Buitrago, W., Settleman, J., and Rosen, J.M. p190-B RhoGAP regulates mammary ductal morphogenesis. Molec. Endocrin. 17:1054-1065, 2003.
2. Frese; K.K., Lee, S.S., Thomas, D.L., Latorre, I., Weiss, R.S., Glaunsinger; B.A., and Javier, R.T.. Selective PDZ protein-dependent stimulation of phosphatidylinositol 3-kinase by the adenovirus E4-ORF1 oncoprotein. Oncogene 22:710-721, 2003.

CONCLUSIONS

The training program in breast cancer supported by the USAMRC has been highly successful in the past eight years. The faculty at Baylor College of Medicine are deeply saddened that USAMRC has ended support of Institutional Training Grants and express the wish that this funding mechanism be reinstituted.

APPENDICES

Table 1.
Publications.

Table 1
Breast Disease Research Group
2002-2003 Schedule
Wednesdays 12:00 p.m., Room M616 (Debakey Bldg.)

APPENDIX 1

DATE	NAME	TITLE	DEPARTMENT
09/18	Orla Conneely, Ph.D.	Professor	Molec. & Cellular Biology
09/25	Era of Hope Meeting		
10/02			
10/09	Rakesh Kumar, Ph.D.	Professor	M.D. Anderson
10/16			
10/23			
10/30	Shaun Zhang, Ph.D.	Assistant Professor	Center for Gene Therapy
11/06	Xiaotao Li, Ph.D.	Post-Doc	Molec. & Cellular Biology
11/13	Mien-Chie Hung, Ph.D.	Professor	M.D. Anderson
11/20	Pepper Schedin, Ph.D.	Scientist	AMC, Denver
11/27	THANKSGIVING WEEK		
12/04	Max Wicha, M.D.	Dir Cancer Center/Prof	Univ of Mich Cancer Center
12/11	San Antonio Meeting		
12/18			
12/25	CHRISTMAS WEEK		
01/01			
01/08	Nathalie Cella, Ph.D.	Post-Doc	Molec. & Cellular Biology
01/15			
01/22	Breast Cancer Think Tank		
01/29	Jeffrey Pollard, Ph.D.	Assoc Dir Cancer Ctr	Albert Einstein College of Med
02/05	Steven M. Townson, Ph.D.	Post-Doc Associate	Breast Center
02/12	Adrian Lee, Ph.D.	Assistant Professor	Breast Center
02/19			
02/26	Isabel Latorre	Graduate Student	Molec. Virology & Microbio.
03/05	Sandy Grimm, Ph.D.	Post-Doc Fellow	Molec. & Cellular Biology
03/12	Monique Rijnkels, Ph.D.	Post-Doc Associate	Molec. & Cellular Biology
03/19	Ashok Venkitaraman	Professor	Univ. of Cambridge
03/26	Bonnie Nannenga	Graduate Student	Molec. Virology & Microbio.
04/02			
04/09	AACR Meeting		
04/16	Grazia Arpino, M.D.	Postdoc Fellow	Breast Center
04/23	Lewis Chodosh, M.D., Ph.D.	Professor	Univ. of Pennsylvania
04/30	Steffi Oesterreich, Ph.D.	Asst. Professor	Breast Center
05/07	Stewart Sell, M.D.	Scientist/Member	Wadsworth Ctr/Ordway Inst.
05/14	Chunhua Lu, M.D.	Postdoc Fellow	Breast Center
05/21	Rachel Schiff, Ph.D.	Asst. Professor	Breast Center
05/28	Catherine Tomasetto, Ph.D.	Research Director	INSERM, Illkirch, France

APPENDIX 2

p190-B RhoGAP Regulates Mammary Ductal Morphogenesis

GEETIKA CHAKRAVARTY, DARRYL HADSELL, WILLIAM BUITRAGO, JEFFREY SETTLEMAN, AND JEFFREY M. ROSEN

Department of Molecular & Cellular Biology (G.C., W.B., J.M.R.), Baylor College of Medicine, and Department of Pediatrics (D.H.), Children's Nutrition Research Center, Houston, Texas 77030; and Massachusetts General Hospital Cancer Center and Harvard Medical School (J.S.), Charlestown, Massachusetts 02129

Previous studies from our laboratory have demonstrated that p190-B RhoGAP (p190-B) is differentially expressed in the Cap cells of terminal end buds (TEBs) and poorly differentiated rodent mammary tumors. Based on these observations we hypothesized that p190-B might play an essential role in invasion of the TEBs into the surrounding fat pad during ductal morphogenesis. To test this hypothesis, mammary development was studied in p190-B-deficient mice. A haploinsufficiency phenotype was observed in p190-B heterozygous mice as indicated by decreased number and rate of ductal outgrowth(s) at 3, 4, and 5 wk of age when compared with their wild-type littermates. This appeared to result from decreased proliferation in the Cap cells of the TEBs, a phenotype remarkably similar to that observed previously in IGF-I receptor null mammary epithelium. Furthermore, de-

creased expression of insulin receptor substrates 1 and 2 were observed in TEBs of p190-B heterozygous mice. These findings are consistent with decreased IGF signaling observed previously in p190-B^{-/-} mouse embryo fibroblasts. To further assess if this defect was cell autonomous or due to systemic endocrine effects, the mammary anlagen from p190-B^{+/+}, p190-B^{+/-}, and p190-B^{-/-} mice was rescued by transplantation into the cleared fat pad of recipient Rag1^{-/-} mice. Surprisingly, as opposed to 75–80% outgrowths observed using wild-type donor epithelium, only 40% of the heterozygous and none of the p190-B^{-/-} epithelial transplants displayed any outgrowths. Together, these results suggest that p190-B regulates ductal morphogenesis, at least in part, by modulating the IGF signaling axis. (*Molecular Endocrinology* 17: 1054–1065, 2003)

EPITHELIAL-STROMAL INTERACTIONS PLAY a critical role in ductal morphogenesis, lobuloalveolar development, and tissue remodeling during involution (1). In the virgin mammary gland, extracellular matrix (ECM) modifications influence ductal branching, end bud development, and epithelial proliferation. The signals propagated by ECM interactions with integrin receptors result in the activation of a number of signaling pathways, among which the activation of Rho family of small GTP-binding proteins play an important role in regulating the formation of focal adhesions and the organization of the actin cytoskeleton (2–4).

ECM interactions directly facilitate invasion of a highly proliferative structure called the terminal end bud (TEB) into the surrounding fat pad. They are composed of an outer layer of highly proliferative cells called the Cap cells, and a multilayered inner mass containing body cells, some of which undergo apoptosis to give rise to the hollow mammary ducts (5). The Cap cell layer contains a pleuripotent stem cell

population that can give rise to intermediate, luminal, and myoepithelial cells of the advancing duct (6–9). Because of their high proliferative potential, these cells are also believed to be the targets of carcinogenesis (10). Although morphological changes in TEBs that lead to the arborization of the ductal system have been well documented, the genes that facilitate invasion of the TEBs remain elusive. In recent years, it has been demonstrated that both IGF-I and IGF-I receptor (IGF-IR) play a major role in TEB formation and elongation (11, 12).

To identify genes that might be preferentially expressed in TEBs, differential-display PCR was originally employed to distinguish genes that were preferentially expressed in TEBs as compared with the midgland and stromal tissue fractions of the nulliparous Wistar-Furth rats. Interestingly, one of the clones identified in this screen was a new member of the RhoGAP family of proteins called p190-B. Because RhoGAPs have been shown to transduce signals from the ECM to the nucleus, it appeared to be a likely candidate to play a role in TEB invasion. Accordingly, using *in situ* hybridization, p190-B expression was observed to be highest in the highly proliferative, outer cap cell layer of the TEB. Ducts, alveolar buds, and stroma all expressed p190-B but at much reduced

Abbreviations: Brdu, Bromodeoxyuridine; ECM, extracellular matrix; FITC, fluorescein isothiocyanate; GAP, GTPase-activating protein; IF, immunofluorescence; IGF-IR, IGF-I receptor; IHC, immunohistochemistry; IRS-1, insulin receptor substrate 1; MEF, mouse embryo fibroblast; RT, room temperature; TEB, terminal end bud.

levels. These findings were corroborated by Northern analysis, which detected the highest level of p190-B expression in the virgin mammary gland declining with pregnancy and lactation, suggesting again that p190-B might play a critical role in ductal morphogenesis during virgin mammary gland development (13).

p190-B is a member of RhoGAP family of proteins and is recruited to the sites of integrin clustering. It encodes a protein with an N-terminal GTPase domain and a C-terminal RhoGAP domain that stimulates the intrinsic GTPase activity of Rho, Rac, and cdc-42, thereby functioning as a negative regulator of their signal-transducing activity. These proteins are conserved from flies to humans. p190-B shares some features in common with several members of the Ras, Rab, Ral, and Rho family of GTPases, but it is most closely related to p190-A, sharing 51% amino acid identity (14). These two genes have been mapped to two different chromosomes, suggesting they diverged early in evolution and may have distinct functions (15).

Rho GTPases are key regulators of a wide range of physiological processes (16, 17). Hence, their spatio-temporal expression is tightly regulated through the opposing actions of guanine nucleotide exchange factors, and the GTPase-activating proteins (GAPs) like the p190RhoGAPs. Studies with p190-A and p190-B null mice have revealed that maintaining a tight spatio-temporal regulation of these genes is critical for normal embryonic development. Loss of p190-RhoGAP results in perinatal lethality due to pleural defects, e.g. p190-A null mice die of severe defects in eye development, formation of the corpus callosum, and neural tube closure (18), whereas p190-B null mice exhibit differentiation defects in the brain and thymus (19).

Despite convincing evidence supporting their role in normal embryonic development and its expression in the Cap cells of the TEBs, the exact function of p190-B signaling in postnatal mammary gland development has not been investigated. Accordingly, the role of p190-B was studied in prepubescent and pubescent mice that were either heterozygous or wild type at the p190-B locus. A haploinsufficiency phenotype was observed in p190-B heterozygous mice as indicated by decreased number and rate of ductal outgrowth(s) at 3, 4, and 5 wk of age when compared with their wild-type littermates. This appeared to result from decreased proliferation in the Cap cells of the TEBs, a phenotype remarkably similar to that observed previously in IGF-IR null mammary epithelium. Accordingly, decreased expression of insulin receptor substrate (IRS)-1 and IRS-2 was observed in TEBs of p190-B heterozygous mice. This was consistent with decreased IGF signaling observed previously in p190-B knockout mouse embryo fibroblasts (MEFs) (19). To further assess whether this defect was cell autonomous or due to systemic endocrine effects, the mammary anlagen from p190-B^{+/+}, p190-B^{+/-}, and p190-B^{-/-} mice was rescued by transplantation into the cleared fat pad of recipient Rag1^{-/-} mice. Surprisingly, as opposed to 75–80% outgrowths observed

using wild-type donor epithelium, only 40% of the heterozygous and none of the p190-B^{-/-} epithelial transplants displayed outgrowths. Together, these results suggest that p190-B regulates ductal morphogenesis, at least in part, by modulating the IGF-signaling axis.

RESULTS

Deletion of a Single Functional Allele of p190-B Is Sufficient to Retard Ductal Morphogenesis

Examination of mature p190-B heterozygous females revealed no apparent defects at most stages of mammary gland development. The heterozygous females were viable, gave birth to normal-sized litters, and nursed their young. Examination of whole mounts of the mammary gland from mature virgin, midpregnant, and lactating mice did not reveal any apparent differences in wild-type and heterozygous mice (data not shown). However, because differential expression of p190-B was observed previously in the Cap cell layer of the TEBs, we hypothesized that deletion of one p190-B allele might influence the rate of ductal outgrowth into the surrounding fat pad in prepubescent and/or early pubescent mice. To explore this possibility, whole-mount analysis was employed to compare the extent of ductal outgrowth in sister pairs of wild-type and heterozygous virgin females at prepubertal and early pubertal stages of development. As seen in Fig. 1A, p190-B heterozygous females exhibited significantly retarded ductal growth at 3, 4, and 5 wk of age when compared with their wild-type littermates. To obtain a quantitative measure of the defect, morphometric analysis was performed on the whole-mount images captured using a charge-coupled device camera. Both the extent of outgrowth and the ratio of the area occupied by the ducts to that of the entire fat pad were analyzed. Two-way ANOVA was used to measure the effect of age, genotype, and the interaction between the two on the extent of ductal outgrowth. Using the lymph node as the reference, both age ($P < 0.001$) and genotype ($P < 0.001$) revealed statistically significant differences on ductal outgrowth, whereas the interaction between age and genotype did not reach statistical significance ($P > 0.1$), suggesting that the genotype had an independent influence on extent of ductal outgrowth in the heterozygous group of mice. When individual time points were analyzed for differences in ductal outgrowth, a dramatic reduction in growth was noted in 3-, 4-, and 5-wk-old mice [$P < 0.05$ (adjusted), t test with equal variance, Fig. 1B]. Next, two-way ANOVA was used to measure the effect of age and genotype (and interaction between the two) on the capacity of wild-type and heterozygous epithelium to fill the fat pad. These analyses also revealed a statistically significant influence of age ($P < 0.001$) and the genotype of the mice, i.e. heterozygous mice had significantly reduced capacity

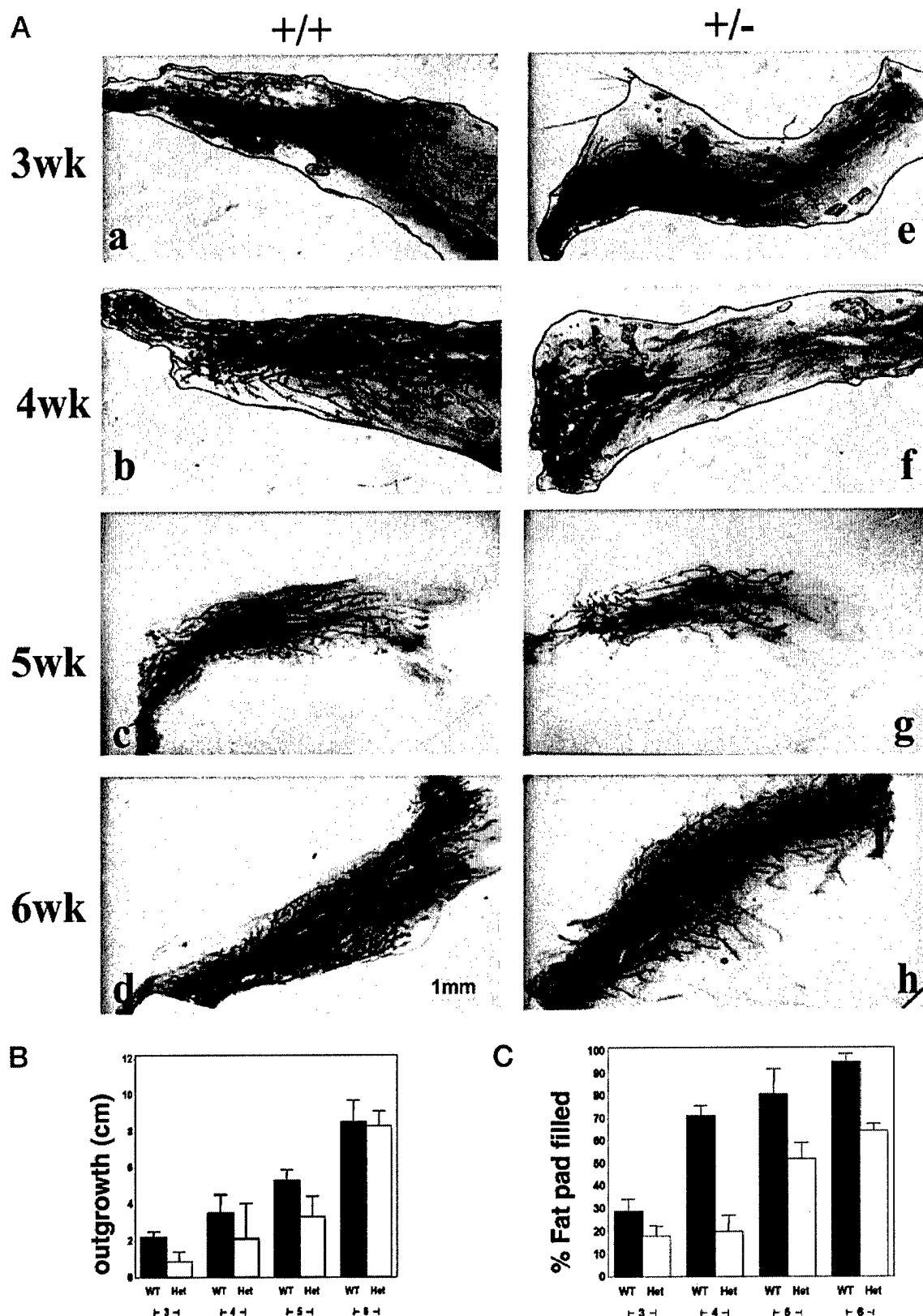


Fig. 1. Haploinsufficiency at the *p190-B* Locus Delays Early Postnatal Development

A, Mammary glands from sister pairs of 3-, 4-, 5-, and 6-wk-old wild-type (a, b, c, and d, respectively) and *p190-B* heterozygous (e, f, g, and h, respectively) mice were whole mounted to analyze the extent of ductal outgrowth. This defect was partially rescued

to fill the fat pad when compared with wild-type mice ($P < 0.001$). This trend continued to be statistically significant at all ages when the data were analyzed for individual time points [$P < 0.002$ (adjusted) at 3, 4, 5, and 6 wk of age, respectively; t test with equal variance, Fig. 1C]. All the above results clearly indicate that p190-B is essential for ductal morphogenesis.

Loss of One Allele of p190-B Phenocopies the Proliferation Defect in the Cap Cell Layer of IGF-IR^{-/-} Mice

To determine whether the retarded ductal development of p190-B^{+/-} was due to differences in the rate of proliferation in TEBs among the two genotypes, both the overall level of proliferation in the TEBs and proliferation in the two outer most cell layers were quantitated by analyzing the number of cells labeled with bromodeoxyuridine (BrdU) during a 2-h pulse. Cells in S phase were detected by IHC using a peroxidase-labeled anti-BrdU antibody. The average level of proliferation in the TEBs at 4–5 wk of age varied considerably, and ranged from 22–27% in both the heterozygous and wild-type mice, similar to values reported previously (5, 11). It was, therefore, difficult to obtain statistically significant differences in the overall level of proliferation in TEBs among the two genotypes. However, as evident from Fig. 2A (compare panel a and c with b and d), proliferation in the Cap cell layer of p190-B^{+/-} mice was dramatically reduced. Although the difference in rate of proliferation in the two outer most cell layers of the TEBs of heterozygous ($30.48\% \pm 6.96$, mean \pm SEM) and the wild type ($35.35\% \pm 5.52$, mean \pm SEM) mice at 4 wk of age was not significant ($P > 0.55$), this difference was highly statistically significant [$P = 0.009$ (unadjusted), $P = 0.017$ (adjusted), t test with equal variance, Fig. 2B] between 5-wk-old heterozygous ($5.21\% \pm 1.75$, mean \pm SEM) and wild-type mice ($29.09\% \pm 6.77$, mean \pm SEM). This difference was also apparent in ANOVA where both age ($P < 0.03$) and genotype ($P < 0.02$) had statistically significant influences on rate of proliferation in the Cap cell layer, while the interaction among the two was not ($P > 0.1$). This was similar to what has been observed previously in mammary transplants from IGF-IR null as compared with wild-type mice, which also displayed a marked decrease in

the level of proliferation in the cap cells of TEBs (Fig. 2A, compare panels e and f) (11). These results are also consistent with recent studies (19) suggesting a possible role of p190-B in mediating the cross-talk between IGF and ECM signaling.

Reduced IRS-1 and IRS-2 Expression in p190-B^{+/-} Mice

The reduction in Cap cell proliferation in both the p190-B^{+/-} mice and the IGF-IR null transplants prompted an investigation of the immediate downstream targets of the IGF-I signaling pathway, *i.e.* insulin receptor substrate proteins, IRS-1 and IRS-2, in p190-B^{+/-} mice. IRS-1 has been shown previously to be targeted for proteasome-mediated degradation as a function of Rho-kinase-mediated phosphorylation in p190-B null MEFs (19). Using IHC, the expression levels of IRS-1 and IRS-2 were compared between the two genotypes. As has been observed previously (20), IRS-1 expression was detected as diffuse, predominantly cytoplasmic staining only in the body cells of the TEBs both in p190-B^{+/-} mice and p190-B^{+/+} mice. No such staining was observed in the TEBs in IRS-1 null mice (20). In contrast, IRS-2 expression was detected in both body cells and in the Cap cell layer with a characteristic ring-like staining pattern around the cell periphery. Both IRS-1 and IRS-2 levels were reduced in p190-B^{+/-} mice as compared with their wild-type littermates. In addition, the ring-like staining pattern of IRS-2 was not apparent in both the body cells and the Cap cell layer of p190-B^{+/-} females (as indicated by arrows in Fig. 3). These results further support a possible interaction between these two pathways that regulates ductal morphogenesis.

Reduced IRS-2 Levels May Account for Lack of Proliferation in the Cap Cell Layer

Because reduced levels of either IRS-1 or IRS-2, or both, may influence proliferation in mammary epithelial cells, we next examined whether they colocalized with the proliferating cells and might account for the lack of proliferation in the Cap cell layer of p190-B^{+/-} mice. For these experiments, IRS-1 and IRS-2 were detected using indirect immunofluorescence (IF) with a secondary antibody conjugated to Texas Red, and

in 6-wk-old heterozygotes (compare panels d and h). B, Using lymph node as the reference, length of the ductal outgrowths was recorded in centimeters for 3-, 4-, 5-, and 6-wk-old wild-type (black bar) and heterozygous (white bars) females from 5 \times 7 prints of the photomicrographs (see Materials and Methods). Plot indicates significantly reduced outgrowth at 3-, 4-, and 5-wk time points [$P = 0.04$, $P = 0.04$, and $P = 0.002$ (adjusted), respectively, t test with equal variance]. Values presented are the mean and 95% confidence interval of the mean from five mice per genotype. C, Quantitative measure of the ability of p190-B heterozygous epithelium to fill the fat pad when compared with wild-type epithelium. Statistically significant differences were observed in the reduced ability of heterozygous epithelium to grow out in the 3-wk- ($P \leq 0.002$), 4-wk- ($P \leq 0.000$), 5-wk- ($P \leq 0.0001$), and 6-wk-old ($P \leq 0.0001$) virgins [t test with equal variance]. When compared with wild type (black bar), heterozygous epithelium (white bars) exhibited a 3.0-fold lower ability to grow out in 4-wk-old females. By 5 wk, this difference was reduced to 1.5-fold, and by 6 wk, no major visual differences were apparent among the two genotypes. Values presented are the mean and 95% confidence interval of the mean from five mice per genotype.

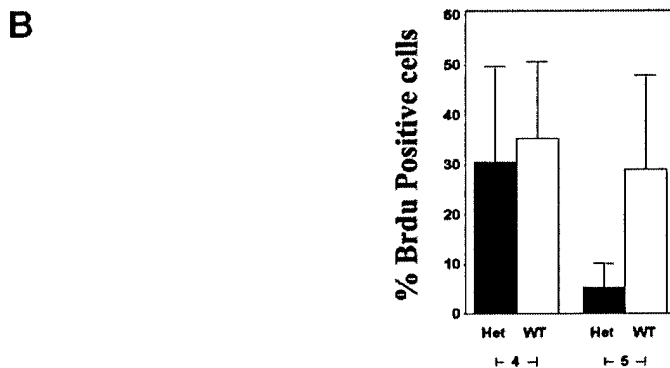
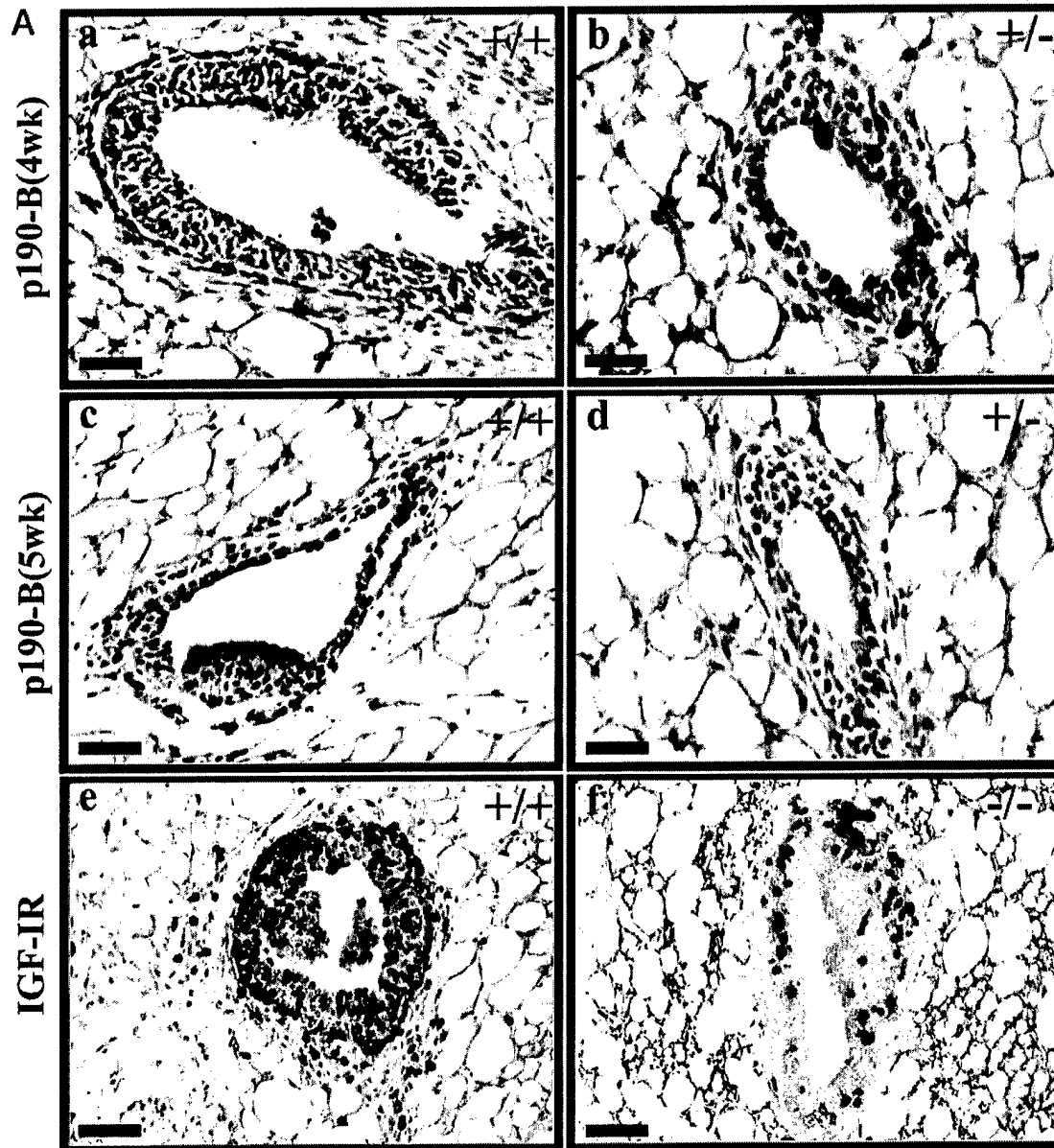


Fig. 2. Delayed Postnatal Development in *p190-B* Heterozygous Mice Results from Reduced Levels of Proliferation in the Cap Cell Layer of TEBS

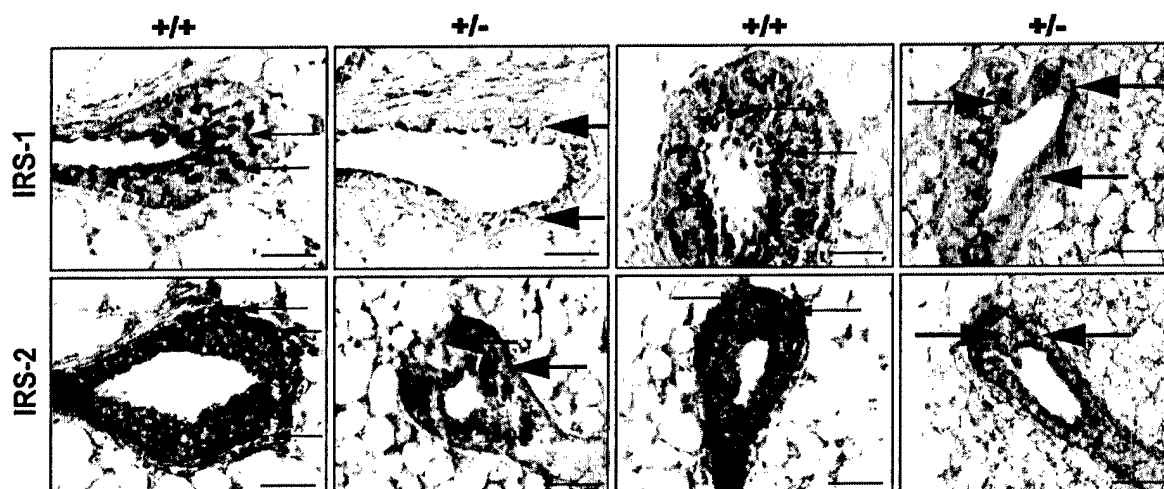


Fig. 3. Reduced IRS-1 and IRS-2 Expression in p190-B Heterozygous Mice

IHC for IRS-1 (top panels) and IRS-2 (bottom panels) in 4-wk-old $p190-B^{+/+}$ and $p190-B^{+/-}$ mice. Thin arrows indicate intense IRS-1 or IRS-2 staining in wild-type mice. Please note the dramatic reduction in IRS-1 and IRS-2 staining in $p190-B^{+/-}$ mice as indicated here with thick arrows. These photomicrographs are representative of images collected from two each of 4-wk- and 5-wk old wild-type and heterozygous mice. Bars, 50 μ m.

proliferation was assessed with a fluorescein isothiocyanate (FITC)-tagged anti-BrdU antibody. The immunofluorescence (IF) results depicted in Fig. 4 are in agreement with those obtained previously by IHC: a reduction of both IRS-1 and IRS-2 expression was observed in $p190-B^{+/-}$ as compared with wild-type mice. However, most of the IRS-1-positive cells did not colocalize with BrdU-positive cells (see Fig. 4A, intense red staining cells marked with a white arrow that is completely lacking in panel B), and IRS-1 expression was not detected in the Cap cells. On the other hand, most IRS-2-positive cells, especially the ones in the Cap cell layer, also stained with the FITC-BrdU antibody, giving rise to yellow (marked with *) or green nuclei with a red border (see Fig. 4C, intense red, ring-like membrane staining all around the green fluorescent BrdU-labeled nuclei, marked with a white arrow). Once again, this staining pattern was lost in the heterozygous mice. Thus, it appears that the decreased expression of IRS-2 in $p190-B^{+/-}$ females correlates best with the decreased proliferation in the Cap cell layer (Fig. 4, B and D).

The Ductal Defect in p190-B Heterozygous Mice Is Cell Autonomous

Because mammary development is controlled by both systemic hormones and locally acting growth factors,

we next asked whether the observed effects on ductal morphogenesis in p190-deficient mice were cell autonomous. However, because $p190-B^{-/-}$ mice are perinatal lethal, embryonic mammary bud transplantation studies were required to address this question. This approach has been employed successfully to rescue the mammary anlagen from a number of gene-targeted mice, such as the pRb-deficient mice, which die as early as embryonic d 12.5 (E12.5) (21). For this assay, both the no. 4 inguinal mammary buds from E16 embryos of the 129Sv/C57 donor mice were rescued by transplantation into the cleared fat pad of $Rag1^{-/-}$ recipient mice. In all three genotypes, mammary anlagen were present at E16, although, as expected, they were smaller in the p190-B null embryos (19). A detailed description of the effects of p190-B on embryonic mammary gland development will be presented elsewhere.

Six weeks after transplantation, the grafts were removed and whole mounted to check the extent of outgrowth. The donor mice were genotyped by PCR after transplantation to ascertain the sex and p190-B status of the embryos. However, to avoid any bias, the mammary outgrowths from all female donors were scored for the extent of outgrowth before evaluating their p190-B status. As seen in representative transplants shown in Fig. 5A, the epithelium from wild-type

A, Representative fields from 4-wk- and 5-wk-old virgin mammary glands of $p190-B^{+/+}$ (a and c), $p190-B^{+/-}$ (b and d) $IGF-IR^{+/+}$ (e), and $IGF-IR^{-/-}$ (f) showing immunohistochemical localization of BrdU-positive cells in TEBs. These panels are depicted here to highlight the differences in the levels of proliferation in the outer cell layers of TEBs of both $p190-B^{+/-}$ and $IGF-IR^{-/-}$ mice. Bars, 50 μ m. B, BrdU-positive cells for both genotypes ($p190-B^{+/+}$ and $p190-B^{+/-}$) were counted and expressed as a ratio of positive nuclei to the total number of nuclei counted in percent. Each slide was scanned to randomly select 10–12 TEBs to count the positive as well as the total number of nuclei in the two outer most cell layers of TEBs. Values represent mean and 95% confidence interval of the mean from five mice per genotype.

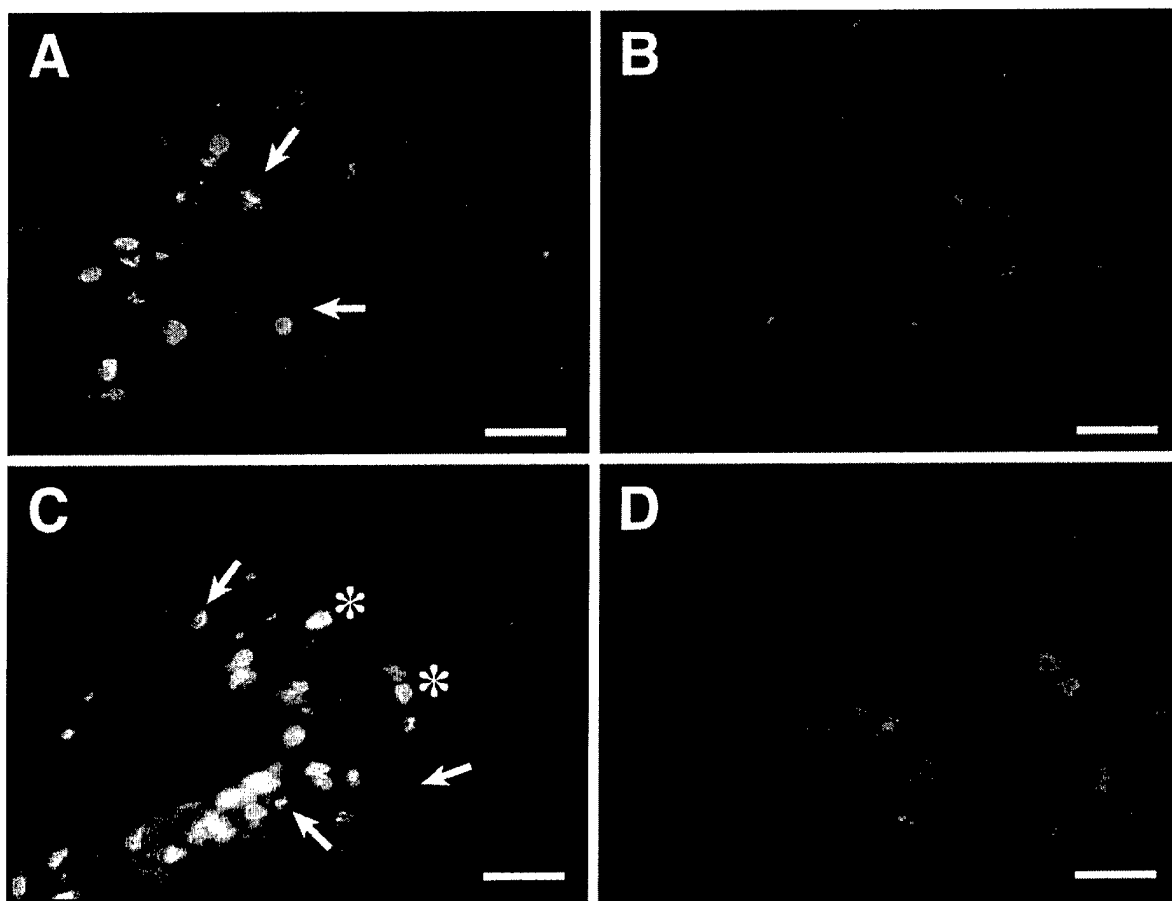


Fig. 4. IRS-2 But Not IRS-1 Staining Correlates with Proliferation in the Cap Cell Layer

Immunofluorescence staining for IRS-1: BrdU (*top panels*: A and B) and IRS-2: BrdU (*bottom panels*: C and D) was performed on sections of wild-type (A and C) or *p190-B*^{-/-} (B and D) glands taken at 4 wk of age. In the wild-type mice, most of the IRS-1 staining was confined to body cells (indicated with *white arrows* in A) and did not colocalize with BrdU-labeled cells. However, most proliferating cells were positive for IRS-2 expression (cells appear *yellow*) as indicated here with * in panel B or show a *thin red ring*-like staining around the *green* nuclei shown here with *arrows*. On the other hand, both IRS-1 and IRS-2 levels were significantly reduced in the *p190-B*^{-/-} mice (B and D) and the correlation with BrdU-positive cells was lost. These photomicrographs are representative of images collected from two each of 4-wk- and 5-wk-old wild-type and heterozygous mice. Bar, 50 μ m.

donors completely filled the fat pad. However, the epithelium transplanted from heterozygous donor mice only partially filled the fat pad, and the epithelium derived from *p190-B* null donors failed to grow out. To quantify the severity of the phenotype, we monitored the take rate (percentage of outgrowths to total tissue grafts) in each of the three subgroups (Fig. 5B). Approximately 75% of the wild-type transplants grew out and filled the fat pad completely, while only 40% of the heterozygous transplants grew out, suggesting that the take rate and extent of outgrowth were dependent on the genotype and not experimental variables. Furthermore, a complete failure of outgrowth was observed in the *p190-B* null transplants. These results indicate that the mammary defect is cell autonomous. Furthermore, even haploinsufficiency exerted a profound effect, and the loss of both alleles of *p190-B* severely affected mammary ductal morphogenesis.

DISCUSSION

Mammary gland development occurs in distinct phases: embryonic, prepubertal, pubertal, pregnancy, lactation, and involution (22). Each of these phases is characterized by distinct morphological changes (23). Because ductal morphogenesis is unique to virgin animals and is the period when they are most susceptible to carcinogenesis, there has been considerable interest in isolating genes that were expressed in this particular window of development. Using differential display and *in situ* hybridization, a novel RhoGAP protein *p190-B* was identified previously in our laboratory (13). It was differentially expressed in TEBs and some rodent mammary tumors. RhoGAPs negatively regulate Rho and promote cell motility and invasion (13, 16, 24). Thus, it was hypothesized that *p190-B* might play a

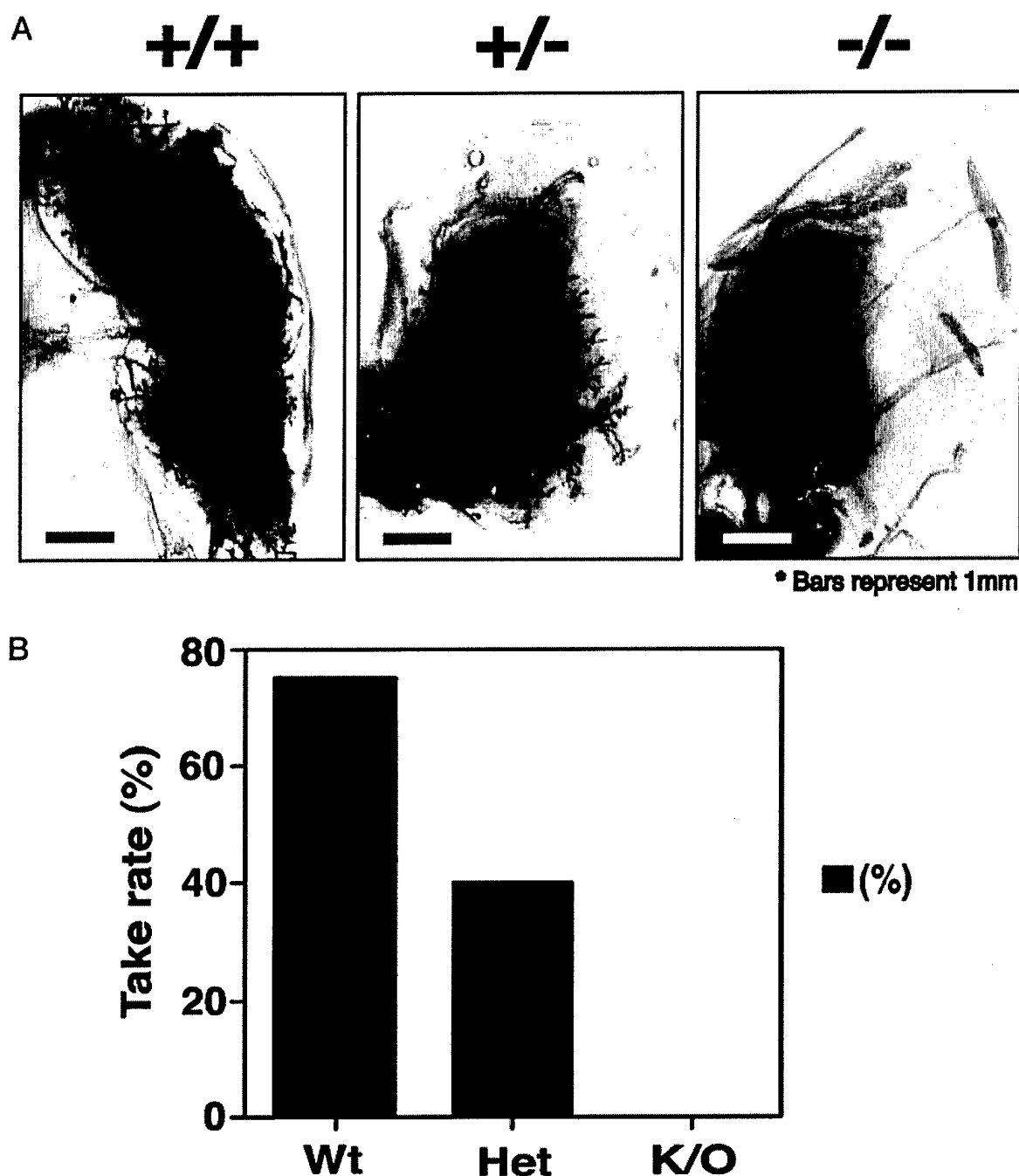


Fig. 5. p190-B RhoGAP Is Essential for Mammary Morphogenesis

A, Whole-mount analysis of mammary glands from *RAG1*^{-/-} mice harboring E16 mammary anlagen transplants. Samples shown here are representative of the phenotype of the respective genotype. Note the difference in the extent of mammary outgrowth in *p190-B* (+/-) and *p190-B* (-/-) transplants, as compared with *p190-B* (+/+) epithelium. *Bar*, 1 mm. **B,** Complete failure of *p190-B*-null embryonic epithelium to give rise to the mammary ductal tree. *Bars* represent the percentage of embryonic buds that successfully repopulate the host fat pad out of the total number of grafts. *n* = 16 for *p190-B* (+/+), *n* = 15 for *p190-B* (+/-), and *n* = 5 for *p190-B* (-/-).

role in TEB invasion into the surrounding fat pad, thereby facilitating ductal morphogenesis. This hypothesis is supported by the observation that the arborized ductal system of virgin mammary gland is

formed as a result of reciprocal communication between the extracellular matrix and the invading TEBs (9). To test our hypothesis, *p190-B* knockout mice were used to examine its functional role in mammary

morphogenesis. Mice lacking one allele of p190-B exhibited retarded ductal morphogenesis. This appears to result from reduced levels of proliferation in the Cap cell layer, in turn resulting, at least in part, from reduced IGF signaling. Surprisingly, deletion of both alleles completely prevented outgrowth of the transplanted mammary anlagen. Thus, p190-B may facilitate ductal morphogenesis by modulating the insulin-signaling pathway through Rho proteins.

Mammary morphogenesis ensues as early as d 10–11 of embryonic development when five pairs of placodes appear on the ventral skin. The growth of the placodes is regulated mainly through reciprocal communication between epithelial cells and the surrounding mesenchyme. Once the epithelial bud is initiated, it induces the formation of the mammary mesenchyme (25). Later, postnatal remodeling of the gland continues in response to systemic and local cues. Although the genetic interactions and signaling pathways regulating postnatal mammary development are starting to be elucidated (21), much less is known about the genes that facilitate invasion of TEBs into the fat pad. Interactions between the estrogen receptor, GH, IGF, and IGF-IR have been shown to be involved in TEB growth and morphogenesis.

In this respect, it was intriguing to see that p190-B was differentially expressed during mammary development and that loss of one allele of p190-B retarded mammary development as visualized in whole mounts (Fig. 1A). However, as evident from the data presented in Fig. 1, B and C, the phenotype is partially rescued by 6 wk of age. One interpretation of these data is that the heterozygous mice have less epithelium at birth, so they grow out more slowly as compared with the wild-type mice, similar to what was observed in the E16 transplants (Fig. 5A). However, at 5–6 wk after birth when they have attained sexual maturity under the influence of increasing estrogen, progesterone, and local IGF-I, a burst of epithelial proliferation may rescue the phenotype so that by 6 wk of age the extent of outgrowth is more or less similar in the heterozygotes and wild-type mice.

Postnatal ductal development of the mammary gland is a unique process in which ductal morphogenesis and ductal elongation go hand in hand and require extensive remodeling of the ECM in response to systemic and local cues. As has been noted in previous studies, the level of proliferation during ductal elongation is considerably higher in the outer Cap cell layer in the TEB, as compared with the cells closest to the lumen that are undergoing apoptosis (5), suggesting that reciprocal communication between the ECM and the Cap cell layer of TEBs may regulate levels of proliferation. Because p190-B is recruited to the sites of integrin clustering and is tyrosine phosphorylated, one can speculate that p190-B may modulate ductal morphogenesis by transducing signals from ECM through Rho proteins. This notion is supported by our observation that loss of one allele of p190-B significantly reduced the level of proliferation (Fig. 2) in the

Cap cell layers in the p190-B heterozygous mice when compared with wild-type mice. This hypothesis is further supported by the observation that loss of IRS-2 also correlates with reduced BrdU-labeled cells in the Cap cell layer of the heterozygous mice. Further indirect evidence comes from studies in *Drosophila*. Billuart *et al.* (26) have shown that p190RhoGAP is regulated by integrins and is essential for axon branch stability in *Drosophila*. Additionally, in the mammary gland, laminin has been shown to transduce signals through integrin receptors to the actin cytoskeleton that result in changes in mammary cell shape (27) and affect TEB function. It is tempting to speculate that p190-B RhoGAP may be a critical component of this signaling pathway.

p190-B may also influence ductal morphogenesis by interacting with the IGF-I signaling pathway. Both IHC and IF analyses (Figs. 3 and 4) demonstrated decreased expression of both IRS-1 and IRS-2 in p190-B^{+/-} mice. However, it appears that the decreased expression of IRS-2 in p190-B^{+/-} females correlated best with the decreased proliferation in the Cap cell layer (Fig. 4, B and D). Because IRS-2 appears to be reduced in both the body and the Cap cells, whereas BrdU incorporation was significantly different only in the Cap cells, it is apparent that reduction in IRS-2 levels alone may not be sufficient to directly regulate proliferation. Most likely the Cap cells may respond to the reduction of IRS-2 differently than the body cells, and other factors such as cross-talk with integrin-mediated signal transduction pathways may play a role in regulating TEB proliferation. The later possibility that Cap cells may utilize different signaling mechanisms than the body cells is supported by a recent report from the laboratory of Barcellos-Hoff (28) showing that TGF- β is differentially expressed and activated in the luminal cells of TEBs but is absent from the Cap cells. However, it also cannot be ruled out that IGF-I-regulated signaling through IRS-1 in the body cells may somehow regulate proliferation in the Cap cells via a paracrine mechanism. In either case, it remains to be determined whether reduction, but not complete elimination, of IRS-1 and IRS-2 expression in the TEBs is sufficient to disrupt IGF signaling in the heterozygous mice. This question can be addressed in the future by analyzing ductal morphogenesis in individual and double IRS-1 and IRS-2 knockout mice. However, at present, with a haploinsufficiency phenotype, and not a complete loss of function, it is not feasible to determine whether there is altered IGF signaling from a small population of Cap cells in the TEB. Attempts to quantitate the response of IGF signaling on downstream targets such as AKT and ERK *in situ* using currently existing phospho-specific antibodies in the Cap and body cells of the TEBs have not provided definitive results. Notwithstanding these technical difficulties, the results presented in this study are consistent with recently published observations of Sordella *et al.* (19), who demonstrated that p190-B plays a critical role in regulating the IGF-I signaling pathway

via the modulation of Rho kinase and IRS-1 levels (19) in MEFs derived from p190-B null mice. Thus, loss of p190-B resulted in elevated levels of Rho kinase and increased threonine phosphorylation of IRS-1, leading to proteasome-mediated degradation, decreased IGF-I signaling, and a decrease in phospho-cAMP response element binding protein. Furthermore, cell size also appeared to be affected in the p190-B-deficient embryos, consistent with the smaller size observed in our studies for the mammary anlage. A second connection with IGF signaling is that defects similar to those observed in Cap cell proliferation in IGF-IR-null mammary epithelial outgrowths (11) were seen in the p190-B heterozygotes, suggesting, once again, that p190-B may interact with the IGF-I signaling pathway to regulate ductal morphogenesis. Together, these data suggest that RhoGAP p190-B plays an essential role in ductal morphogenesis and that it might influence Cap cell proliferation and invasion through interaction with both the integrin and IGF-I signaling pathways.

Finally, although the transplantation of the embryonic mammary anlagen was an effective way 1) to circumvent the problem associated with embryonic or perinatal lethal phenotype observed in p190-B mice and 2) to determine the epithelial cell autonomous nature of the decreased rate of ductal outgrowth, this approach still precluded the analysis of postnatal mammary morphogenesis in mice deficient in both alleles of p190-B. Both gain- and loss-of-function experiments will need to be performed using inducible systems to either overexpress p190-B in the mammary gland or floxed alleles with inducible Cre recombinase to permit conditional deletion of this essential gene at different stages of development in a spatiotemporally defined manner. These approaches should help provide additional insight on the role of p190-B in postnatal development. In addition, these models should permit a functional evaluation of the importance of p190-B in mammary tumorigenesis and metastasis.

MATERIALS AND METHODS

Mouse Strains

p190-B-null mice, generated in the laboratory of Dr. Jeffrey Settleman (Harvard Medical School, Cambridge, MA), were maintained on a C57Bl/6 × 129SV background. A heterozygous breeding pair was used to establish a colony in the animal facility at Baylor College of Medicine (Houston, TX). Mice were fed a conventional diet *ad libitum* and maintained at 21–22°C with a 12-h light, 12-h dark cycle. Animal protocols were approved by the Animal Care and Use Committee of Baylor College of Medicine and were conducted in accordance with NIH guidelines. All animals were maintained in accordance with the provisions of the Guide for the Care and Use of Laboratory Animals and the Animal Welfare Act.

Whole Mounts

Whole-mount hematoxylin staining was performed as described by Medina *et al.* (29). Whole mounts were analyzed for growth by measuring the percent fat pad filled by the ductal system of the outgrowth. This was estimated by measuring the area occupied by the ducts divided by the total area of the fat pad, expressed in percent. The analyses were performed using Adobe Photoshop (Adobe Systems, San Jose, CA) and Scion Image (Scion Corp., Frederick, MD) image processing and analysis software. Grayscale TIFF images of whole mounts were captured with a Sony video camera (DXC-151A) and Scion LG3 frame grabber (Scion Corp.) at a resolution of 72 pixels/inch. To quantitate the area occupied by the ductal system and the fat pad, images of whole mounts (magnification, ×6.7) were viewed in Adobe Photoshop and were layered with the grid. The total number of squares overlying these structures provided an approximate measure of the area occupied by them and was used to calculate the ratios. To determine the extent of outgrowth, the whole-mount images were captured as above and printed as 5 × 7 prints. Using lymph node as the reference, the farthest tip of each outgrowth was measured in centimeters, and the mean and 95% confidence interval of the mean were plotted against each genotype.

Immunohistochemistry

Dr. Adrian V. Lee generously provided us the IRS-1 and IRS-2 antibodies for IHC and IF studies. Tissues were fixed with 4% paraformaldehyde, dehydrated through the ethanol series, and paraffin embedded. Five-micrometer sections were baked overnight at 37°C, deparaffinized with xylene, and rehydrated with ethanols. Heat-induced antigen retrieval was performed in 0.1 M Tris-HCl, pH 9.0, for 5 min. Endogenous peroxidase activity was blocked by incubating the sections in 5% hydrogen peroxide solution for 5 min. All incubations were performed at room temperature, and all washing was performed with TBST (0.15 M NaCl; 0.01 M Tris-HCl, pH 7.4; 0.05% Tween 20) unless otherwise stated. Endogenous biotin was blocked using the Avidin/Biotin blocking kit according to the manufacturer's instructions (Vector Laboratories, Inc., Burlingame, CA). Slides were then incubated with IRS-1 antibody (1:800 dilution in Tris-buffered saline + 1% BSA) or IRS-2 antibody (1:800 dilution in Tris-buffered saline + 1% BSA) for 1 h, biotinylated secondary antibody (1:250) for 30 min, and then horseradish peroxidase-labeled avidin (1:200) for 30 min. As a negative control, slides were incubated with purified rabbit immunoglobulin (The Jackson Laboratory, Bar Harbor, ME). Detection was achieved by incubation with diaminobenzidine (DAKO Corp., Carpinteria, CA) for 2 min. Slides were counterstained with 0.05% methylene green for 30 sec, dehydrated, and mounted using Permount (Sigma, St. Louis, MO). Hadsell *et al.* (30) have shown previously that IRS-1 IHC on lactating mammary glands reveals a specific cytoplasmic staining that was absent in control IgG incubations. Both antibodies have been shown to be very specific by immunoblotting, giving a single band at 175 and 185 kDa, respectively. In addition, IRS-1 antibody did not show any staining on IRS-1 null mammary tissue (Dr. A. V. Lee, personal communication). BrdU IHC was performed essentially using the BrdU *in situ* detection kit (catalog no. 550803) as per the manufacturer's instruction (BD Pharmingen, San Diego, CA).

Immunofluorescent Detection of IRS-1, IRS-2, and BrdU

Sections were dewaxed and subjected to microwave antigen retrieval in 10 mM citrate buffer, pH 6.0. After blocking in 5% BSA/0.5% Tween-20 for 4 h at room temperature (RT), sections were incubated overnight with IRS-1 or IRS-2 and anti-BrdU-FITC-conjugated antibody (1:5; Becton Dickinson and

Co., Franklin Lakes, NJ) in blocking solution at RT. Slides were washed in PBS and incubated for 30 min to 1 h in Texas red-conjugated goat antirabbit polyclonal antiserum (1:1000, catalog no. T-6391, Molecular Probes, Inc., Eugene, OR) at RT. After washing off the secondary antibody, slides were mounted in Vectashield + 4',6-diamidino-2-phenylindole (DAPI) medium (Vector Laboratories, Inc.). All procedures were carried out in the dark to prevent fluorochrome quenching.

Mammary Tissue Transplantation

Heterozygous males and females were bred to generate wild-type ($p190-B^{+/+}$), heterozygous ($p190-B^{+/-}$), and null ($p190-B^{-/-}$) donor embryos for mammary transplants. The appearance of a vaginal plug was considered to mark d 0 of gestation. On d 16 of pregnancy, embryos were harvested by cesarean section and kept on ice in Hanks' balanced salt solution until dissection. As $p190-B$ heterozygotes were in a mixed background, immunocompromised $RAG1^{-/-}$ mice were employed as hosts to avoid graft rejection. In addition, unlike nude or skid mice, $RAG1^{-/-}$ mice have a more normal hormonal milieu, making them an ideal host for mammary transplant studies that heavily depend on systemic hormones as well as local growth factors. Three-week-old $RAG1^{-/-}$ mice were directly purchased from The Jackson Laboratory. Both the no. 4 mammary glands of the 3-wk-old $RAG1^{-/-}$ recipients were cleared of any endogenous epithelium (31). The no. 4 inguinal mammary buds from each donor embryo were located under a dissecting scope, surgically removed using a fine clipping forceps, and implanted into an incision in the cleared fat pad of the recipient gland. The mammary buds were transplanted along with the overlying skin. Mammary gland outgrowths were analyzed 6 wk after transplantation by whole-mount staining (25). Embryos were genotyped by PCR to ascertain their sex and $p190-B$ status. The following primer sets (forward, 5'-GGT TCTCACTAGAACGG-3'; reverse, 5'-TAATGATAGGCGGATCCC-3'; neo reverse, 5'-CGGTG-GATGTGGAATGTG-3') were used to amplify $p190-B$ wild-type and mutant alleles. The sex of the embryos was established by PCR on embryo DNA by amplification of the sex-determining region of the Y chromosome (SRY gene). The forward SRY primer was 5'-CGCCCATGAATGCATT-TATG-3', and the reverse primer was 5'-CCTCCGATGAG-GCTGATAT-3'. PCR cycling was for 1 min at 94°C, 2 min at 55°C, and 2 min at 72°C, for 30 cycles. Mouse β -casein primers from exon 7 (MBC7F: 5'-GATGTGCTCCAGGCTA-AAGTT-3'; MBC7R: 5'-AGAAACGGAATGTTGTGGAGT-3') were used as internal positive controls for the latter PCRs.

Statistical Analysis

Data for extent of outgrowth, percent fat pad filled, and BrdU incorporation were summarized with means, SEMs, and 95% confidence intervals. Two-way ANOVA was used to test for main effects of age, genotype, and interaction. In addition, two sample *t* tests were used to compare genotypes at individual time points. *P* values were adjusted for multiple comparisons using the step-down approach to the Sidak method (32). For the BrdU incorporation experiments, the test for homogeneity of variances was significant, and the data were also analyzed using the arcsin square root transform to equalize variances. The results were essentially unchanged (data not shown), and only the untransformed results are reported. Data were analyzed using the software SAS 8.02 (SAS Institute, Inc., Cary, NC).

Acknowledgments

We thank the following persons from the Breast Center, Baylor College of Medicine: Dr. Susan Galloway Hilsenbeck

for all the statistical analyses; Dr. Adrian Lee for sharing IRS-1 and IRS-2 antibodies; Dr. Allred and Dr. Mohsin for help with IHC studies; and Nicole Lawrence for technical assistance with immunoblotting and phospho-specific antibody staining.

Received December 18, 2002. Accepted March 5, 2003.

Address all correspondence and requests for reprints to: Dr. Jeffrey M. Rosen, Department of Molecular and Cellular Biology, Baylor College of Medicine, Houston, Texas 77030. E-mail: jrosen@bcm.tmc.edu.

This work was supported by United States Army Medical Research and Materiel Command DAMD-17-99-1-9073 and R01-CA-64255 postdoctoral support (to G.C.) and R01-DK-052197-06A1 (to D.H.).

REFERENCES

1. Bissell MJH 1987 Form and function in the mammary gland: the role of extracellular matrix. New York: Plenum Publishing Corp.
2. Keely P, Parise L, Juliano R 1998 Integrins and GTPases in tumour cell growth, motility and invasion. *Trends Cell Biol* 8:101–106
3. Leeuwen FN, Kain HE, Kammen RA, Michiels F, Kranenburg OW, Collard JG 1997 The guanine nucleotide exchange factor Tiam1 affects neuronal morphology; opposing roles for the small GTPases Rac and Rho. *J Cell Biol* 139:797–807
4. Mercurio AM, Rabinovitz I, Shaw LM 2001 The $\alpha 6 \beta 4$ integrin and epithelial cell migration. *Curr Opin Cell Biol* 13:541–545
5. Humphreys RC, Krajewska M, Kmacik S, Jaeger R, Weiher H, Krajewski S, Reed JC, Rosen JM 1996 Apoptosis in the terminal endbud of the murine mammary gland: a mechanism of ductal morphogenesis. *Development* 122:4013–4022
6. Pitelka DR, Hamamoto ST 1977 Form and function in mammary epithelium: the interpretation of ultrastructure. *J Dairy Sci* 60:643–654
7. Smith GH, Chapko G 2001 Mammary epithelial stem cells. *Microsc Res Tech* 52:190–203
8. Welm BE, Tepera SB, Venezia T, Graubert TA, Rosen JM, Goodell MA 2002 Sca-1(pos) cells in the mouse mammary gland represent an enriched progenitor cell population. *Dev Biol* 245:42–56
9. Williams JM, Daniel CW 1983 Mammary ductal elongation: differentiation of myoepithelium and basal lamina during branching morphogenesis. *Dev Biol* 1983 97:274–290
10. Russo J, Russo IH 1987 Biological and molecular bases of mammary carcinogenesis. *Lab Invest* 57:112–137
11. Bonnette SG, Hadsell DL 2001 Targeted disruption of the IGF-I receptor gene decreases cellular proliferation in mammary terminal end buds. *Endocrinology* 142: 4937–4945
12. Kleinberg DL, Feldman M, Ruan W 2000 IGF-I: an essential factor in terminal end bud formation and ductal morphogenesis. *J Mammary Gland Biol Neoplasia* 5:7–17
13. Chakravarty G, Roy D, Gonzales M, Gay J, Contreras A, Rosen JM 2000 P190-B, a Rho-GTPase-activating protein, is differentially expressed in terminal end buds and breast cancer. *Cell Growth Differ* 11:343–354
14. Burbelo PD, Miyamoto S, Utani A, Brill S, Yamada KM, Hall A, Yamada Y 1995 p190-B, a new member of the Rho GAP family, and Rho are induced to cluster after integrin cross-linking. *J Biol Chem* 270:30919–30926
15. Burbelo PD, Finegold AA, Kozak CA, Yamada Y, Takami H 1998 Cloning, genomic organization and chromosomal

- assignment of the mouse p190-B gene. *Biochim Biophys Acta* 1443:203–210
16. Schmitz AA, Govek EE, Bottner B, Van Aelst L 2000 Rho GTPases: signaling, migration, and invasion. *Exp Cell Res* 261:1–12
 17. Hall A 1998 Rho GTPases and the actin cytoskeleton. *Science* 279:509–514
 18. Brouns MR, Matheson SF, Hu KQ, Delalle I, Caviness VS, Silver J, Bronson RT, Settleman J 2000 The adhesion signaling molecule p190 RhoGAP is required for morphogenetic processes in neural development. *Development* 127:4891–4903
 19. Sordella R, Classon M, Hu KQ, Matheson SF, Brouns MR, Fine B, Zhang L, Takami H, Yamada Y, Settleman J 2002 Modulation of CREB activity by the Rho GTPase regulates cell and organism size during mouse embryonic development. *Dev Cell* 2:553–565
 20. Lee AV, Zhang JP, Ivanova M, Bonnette S, Oesterreich S, Rosen JM, Grimm S, Hovey RC, Vonderhaar BK, Kahn CR, Torres D, George J, Mohsin S, Allred DC, Hadsell DL, Developmental and hormonal signals dramatically alter the localization and abundance of insulin receptor substrate proteins in the mammary gland. *Endocrinology*, in press
 21. Robinson GW, Wagner KU, Hennighausen L 2001 Functional mammary gland development and oncogene-induced tumor formation are not affected by the absence of the retinoblastoma gene. *Oncogene* 20:7115–7119
 22. Hennighausen L, Robinson GW 2001 Signaling pathways in mammary gland development. *Dev Cell* 1:467–475
 23. Daniel CW, Smith GH 1999 The mammary gland: a model for development. *J Mammary Gland Biol Neoplasia* 1:3–8
 24. Zrihan-Licht S, Fu Y, Settleman J, Schinkmann K, Shaw L, Keydar I, Avraham S, Avraham H 2000 RAFTK/Pyk2 tyrosine kinase mediates the association of p190 RhoGAP with RasGAP and is involved in breast cancer cell invasion. *Oncogene* 19:1318–1328
 25. Robinson GW, Karpf AB, Kratochwil K 1999 Regulation of mammary gland development by tissue interaction. *J Mammary Gland Biol Neoplasia* 4:9–19
 26. Billuart P, Winter CG, Maresh A, Zhao X, Luo L 2001 Regulating axon branch stability. The role of p190 RhoGAP in repressing a retraction signaling pathway. *Cell* 107:195–207
 27. Streuli CH, Edwards GM 1998 Control of normal mammary epithelial phenotype by integrins. *J Mammary Gland Biol Neoplasia* 3:151–163
 28. Ewan KB, Shyamala G, Ravani SA, Tang Y, Akhurst R, Wakefield L, Barcellos-Hoff MH 2002 Latent transforming growth factor- β activation in mammary gland: regulation by ovarian hormones affects ductal and alveolar proliferation. *Am J Pathol* 160:2081–2093
 29. Medina D, Kittrell FS, Liu YJ, Schwartz M 1993 Morphological and functional properties of TM preneoplastic mammary outgrowths. *Cancer Res* 53:663–667
 30. Hadsell DL, Alexeenko T, Klemintidis Y, Torres D, Lee AV 2001 Inability of overexpressed des(1–3)human insulin-like growth factor I (IGF-I) to inhibit forced mammary gland involution is associated with decreased expression of IGF signaling molecules. *Endocrinology* 142:1479–1488
 31. DeOme KB, Faulkin Jr LJ, Bern HA, Blair PE 1959 Development of mammary tumors from hyperplastic alveolar nodules transplanted into gland-free mammary fat pads of female C3H mice. *Cancer Res* 19:515–520
 32. Westfall PH, Young SS 1993 Resampling based multiple testing. New York: John Wiley & Sons, Inc.



Selective PDZ protein-dependent stimulation of phosphatidylinositol 3-kinase by the adenovirus E4-ORF1 oncoprotein

Kristopher K Frese¹, Siu Sylvia Lee^{†1}, Darby L Thomas^{#1}, Isabel J Latorre¹, Robert S Weiss^{†1}, Britt A Glaunsinger^{\$1} and Ronald T Javier^{1,2}

¹Department of Molecular Virology and Microbiology, Baylor College of Medicine, Houston, TX 77030, USA

While PDZ domain-containing proteins represent cellular targets for several different viral oncoproteins, including human papillomavirus E6, human T-cell leukemia virus type 1 Tax, and human adenovirus E4-ORF1, the functional consequences for such interactions have not been elucidated. Here we report that, at the plasma membrane of cells, the adenovirus E4-ORF1 oncoprotein selectively and potently stimulates phosphatidylinositol 3-kinase (PI3K), triggering a downstream cascade of events that includes activation of both protein kinase B and p70S6-kinase. This activity of E4-ORF1 could be abrogated by overexpression of its PDZ-protein targets or by disruption of its PDZ domain-binding motif, which was shown to mediate complex formation between E4-ORF1 and PDZ proteins at the plasma membrane of cells. Furthermore, E4-ORF1 mutants unable to activate the PI3K pathway failed to transform cells in culture or to promote tumors in animals, and drugs that block either PI3K or p70S6-kinase inhibited E4-ORF1-induced transformation of cells. From these results, we propose that the transforming and tumorigenic potentials of the adenovirus E4-ORF1 oncoprotein depend on its capacity to activate PI3K through a novel PDZ protein-dependent mechanism of action.

Oncogene (2003) 22, 710–721. doi:10.1038/sj.onc.1206151

Keywords: adenovirus; E4-ORF1; PDZ; PI3K; oncoprotein

Introduction

Human adenovirus type 9 (Ad9) is distinct among tumorigenic adenoviruses (Ads) in eliciting exclusively estrogen-dependent mammary tumors in rats (Javier

et al., 1991) and in having as its primary oncogenic determinant the E4 region-encoded ORF1 (E4-ORF1) protein (Javier, 1994), rather than the E1 region-encoded E1A and E1B proteins (Thomas *et al.*, 1999). In addition, a recombinant E1 region-deleted Ad5 vector engineered to ectopically express Ad9 E4-ORF1 induces solely mammary tumors, identical to those produced by Ad9, whereas the parental virus vector fails to generate tumors of any kind (Thomas *et al.*, 2001). Thus, in animals, E4-ORF1 also largely determines the capacity of Ad9 to target tumorigenesis specifically within cells of the mammary gland.

Mutational analyses of the 125-amino-acid (aa) residue E4-ORF1 protein have identified three discrete regions (I, II, and III) essential for its cellular transforming functions (Weiss *et al.*, 1997a). Although activities have not yet been ascribed to regions I and II, region III at the extreme carboxyl-terminus of E4-ORF1 defines a functional PDZ domain-binding motif that mediates interactions with a select group of cellular PDZ domain-containing proteins. PDZ domains are protein–protein interaction modules found in cellular factors that typically function in signal transduction (Sheng and Sala, 2001). To date, we have identified four E4-ORF1-associated PDZ proteins as the multi-PDZ protein MUPP1 (Lee *et al.*, 2000) and the three membrane-associated guanylate kinase (MAGUK)-family proteins DLG, MAGI-1, and ZO-2 (Lee *et al.*, 1997; Glaunsinger *et al.*, 2000, 2001). MUPP1 consists of 13 PDZ domains and no other recognizable motifs, whereas the MAGUK proteins contain from three to five PDZ domains, either one SH3 domain or two WW domains, and a yeast guanylate kinase-homology domain. These domain structures comprising numerous protein-binding modules suggest that, like the *Drosophila* multi-PDZ protein InaD (Tsunoda and Zuker, 1999), E4-ORF1-associated PDZ proteins function as scaffolding proteins both to assemble receptors and cytosolic factors into supramolecular complexes and to localize these signaling complexes to the plasma membrane at specialized regions of cell–cell contact (Sheng and Sala, 2001).

High-risk human papillomavirus E6 and human T-cell leukemia virus type 1 Tax oncoproteins also possess PDZ domain-binding motifs at their carboxyl-termini (Lee *et al.*, 1997). These motifs mediate binding to some

*Correspondence: Dr R. Javier, Department of Molecular Virology and Microbiology, Baylor College of Medicine, One Baylor Plaza, Houston, TX 77030, USA; E-mail: rjavier@bcm.tmc.edu

[†]Present addresses: [†]Department of Molecular Biology, Massachusetts General Hospital, Boston, MA 02114; [#]Department of Microbiology, University of Pennsylvania School of Medicine, Philadelphia, PA 19104; ^{\$}Department of Biomedical Sciences, Cornell University, Ithaca, NY 14853; ²Department of Microbiology & Immunology, University of California Medical Center, San Francisco, CA 94143. Received 9 July 2002; revised 21 October 2002; accepted 21 October 2002

E4-ORF1-associated PDZ proteins (Lee *et al.*, 1997, 2000; Glaunsinger *et al.*, 2000) and, moreover, are required for E6-induced transformation of rat 3Y1 fibroblasts (Kiyono *et al.*, 1997) and for Tax-induced reversal of a block to cell-cycle progression caused by overexpression of DLG in mouse 3T3 cells (Suzuki *et al.*, 1999). The latter observation should be interpreted cautiously, however, as DLG expressed at normal physiological levels has not yet been demonstrated to suppress cell-cycle progression in mammalian cells. Thus, while PDZ proteins represent common cellular targets for several different human virus oncoproteins, the functional consequences of these interactions are not yet understood.

As PDZ proteins typically function at the plasma membrane, it is reasonable to hypothesize that viral oncoproteins target these cellular factors to dysregulate cell growth-regulatory signaling pathways originating from this site. Phosphatidylinositol 3-kinase (PI3K) is a key component of one such signaling cascade that normally becomes triggered by activation of tyrosine kinase and heterotrimeric G-protein-coupled membrane receptors (Blume-Jensen and Hunter, 2001). These receptors stimulate the activity of PI3K and its recruitment to the plasma membrane, where this lipid kinase phosphorylates phosphatidylinositides at position D3 of the inositol moiety. The resulting 3,4,5-phosphatidylinositide lipid products then act as second messengers to induce membrane translocation of the serine/threonine protein kinase Akt/protein kinase B (PKB) and stimulation of its kinase activity through phosphorylation of threonine-residue 308 (Thr308) by PDK1 and serine-residue 473 (Ser473) by an undetermined kinase. Activated PKB has been shown to promote both survival and proliferation of cells through its ability to control the activities of multiple downstream effectors, including proapoptotic Forkhead transcription factors, translation and cell-cycle progression regulator p70S6-kinase (S6K), and cyclin-dependent kinase inhibitor p27Kip1 (Yu and Sato, 1999; Medema *et al.*, 2000). A critical antagonist of the PI3K signaling pathway is the tumor-suppressor protein PTEN, a lipid phosphatase that specifically removes the D3 phosphate from 3,4,5-phosphatidylinositide and thereby reverses the action of PI3K (Yamada and Araki, 2001). The presence of *PTEN* mutations in approximately 20% of human cancers and amplification of *PI3K* and *PKB* in some human tumors have established a central role for dysregulated PI3K signaling in the development of human malignancies (Mills *et al.*, 2001).

Our previous results showed that E4-ORF1 sequesters a large fraction of its PDZ-protein targets in the cytoplasm of cells (Glaunsinger *et al.*, 2000, 2001; Lee *et al.*, 2000). We now report that E4-ORF1 likewise complexes with its PDZ-protein targets at the plasma membrane to selectively activate PI3K and that this activity is required for the oncogenic potential of E4-ORF1. In addition to exposing a novel PDZ protein-dependent mechanism for PI3K stimulation, these findings are also significant in revealing for the first

time a physiologically relevant functional consequence for interactions of a viral oncoprotein with its PDZ-protein targets.

Results

Selective stimulation of PI3K by wild-type (wt) but not transformation-deficient mutant E4-ORF1

The fact that cellular PDZ proteins generally function in signal transduction prompted experiments to assess whether E4-ORF1 activates any known signaling factors in cells. We initially focused our attention on a group of such proteins (PI3K, JNK1, β -catenin/TCF, NF κ B, STAT3, and Notch) that have been implicated in transformation (Kimble and Simpson, 1997; Bowman *et al.*, 2000; Tsatsanis and Spandidos, 2000; Uthoff *et al.*, 2001; Vogt, 2001). By comparing their activities in E4-ORF1-expressing versus nonexpressing cells using a variety of approaches, we discovered that E4-ORF1 selectively stimulates PI3K (Figure 1) (unpublished data). For example, the PI3K activity in a CREF rat embryo fibroblast line stably expressing E4-ORF1 (CREF-E4-ORF1) was shown to be 2.5-fold higher than that in normal CREF cells (Figure 1a). This level of activation was comparable to the threefold increase in PI3K activity produced by stimulating CREF cells with the growth factor PDGF and was likewise abolished by the PI3K inhibitor wortmannin (Figure 1a).

The GFP-AH fusion protein (Watton and Downward, 1999), consisting of GFP linked to the pleckstrin-homology (PH) domain of PKB, was exploited to demonstrate similar PI3K stimulation by transiently expressed E4-ORF1 and to reveal the location of this event in cells. Owing to specific binding of this PH domain to PI3K lipid products, GFP-AH translocates from the nucleus/cytoplasm to the membrane upon activation of PI3K in cells. In agreement with results presented in Figure 1a, we demonstrated that, whereas GFP-AH transiently expressed alone exhibits an expected diffuse nuclear and cytoplasmic distribution in 3T3 cells, coexpression with E4-ORF1 causes this fusion protein to accumulate at the plasma membrane in greater than 75% of transfected cells (Figure 1b). This effect was inhibited by wortmannin and also was specific because E4-ORF1 failed to promote membrane translocation of GFP-AH^{R25C} (Figure 1b), which contains a mutant PH domain unable to bind PI3K lipid products (Watton and Downward, 1999).

We extended these results by also examining a collection of E4-ORF1 mutants that either lack focus-forming activity (IIIA, T123D, V125A, IA, IIA, IIB) or exhibit *wt* focus-forming activity (T108S) in CREF cells (Figure 1c) (Weiss *et al.*, 1997a). Transformation-deficient mutants IIIA, T123D, and V125A have region III mutations that inactivate the PDZ domain-binding motif, whereas transformation-deficient mutants IA, IIA, and IIB have region I or II mutations

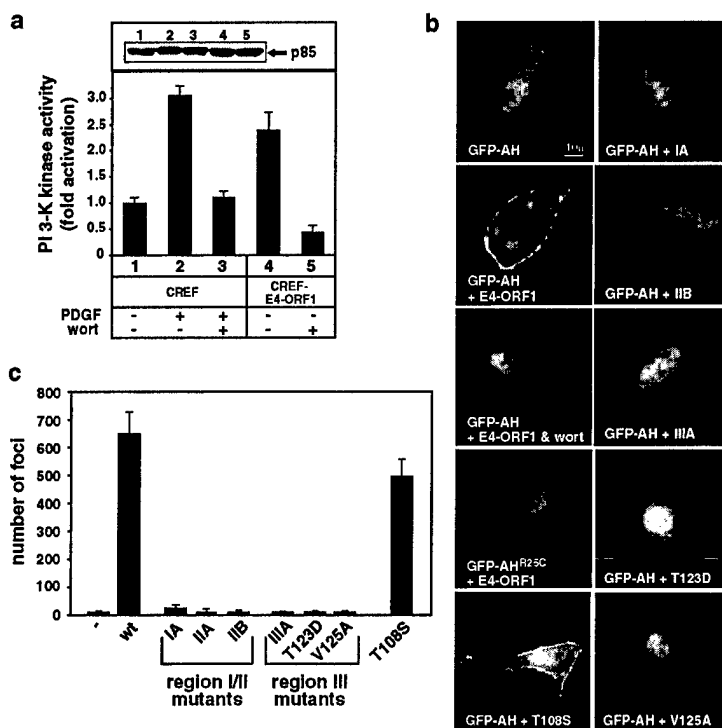


Figure 1 E4-ORF1 activates PI3K. (a) Elevated PI3K activity in E4-ORF1-expressing cells. An equivalent amount of extract from serum-starved CREF or CREF-E4-ORF1 cells was subjected to *in vitro* PI3K assays with PI substrate (bottom) as described in Materials and methods or to immunoblot analyses with anti-p85 antibodies (top). Indicated samples were untreated (–) or treated with 10 ng/ml PDGF and/or 100 nM wortmannin (wort). Results were compiled from three independent experiments. (b) PI3K lipid products accumulate at the plasma membrane of E4-ORF1-expressing cells. NIH 3T3 cells on coverslips in 6-cm dishes were lipofected with pGFP-AH or -AH^{R25C} (0.5 µg each) and pGW1 encoding wt or the indicated mutant E4-ORF1 (50 ng each). Confluent serum-starved cells were visualized by fluorescence microscopy. Indicated cells were pretreated with 100 nM wortmannin (wort). For cells expressing E4-ORF1 mutants unable to activate PI3K, GFP-AH accumulated at variable levels in NIH 3T3 cell nuclei. Therefore, the brighter nuclear GFP-AH signal observed in the cell expressing T123D was not a general finding in these experiments. (c) Focus formation by wt and mutant E4-ORF1 proteins. CREF cells in 10-cm dishes were transfected with empty pJ4Q (–) or pJ4Q encoding wt or the indicated mutant E4-ORF1 (20 µg each) in triplicate. Foci were quantified 3 weeks post-transfection

that do not affect the function of this motif (Weiss and Javier, 1997). The T108S mutation is located outside of the three crucial regions of E4-ORF1. Modeling the E4-ORF1 polypeptide to the crystal structure of the related dUTPase enzyme (Weiss *et al.*, 1997b) predicts that regions I and II lie in close proximity to each other within the native polypeptide (unpublished data), hinting that these sequences contribute to one additional E4-ORF1 functional domain having an undefined activity. Despite exhibiting wt protein expression (unpublished data), all transformation-deficient mutants failed to promote membrane translocation of GFP-AH in cells, whereas the control transformation-proficient mutant T108S behaved similar to wt E4-ORF1 in the assay (Figure 1b). These findings reveal an intimate link between E4-ORF1-mediated cellular transformation and PI3K activation at the plasma membrane and also indicate that both activities are dependent on the PDZ domain-binding motif and an undefined region I/II function of E4-ORF1.

PDZ protein-dependent recruitment of E4-ORF1 to the plasma membrane

The finding that E4-ORF1 caused accumulation of PI3K lipid products at the plasma membrane prompted analyses to investigate whether E4-ORF1 associates with PDZ proteins at this site in cells. In human TE85 cells stably expressing E4-ORF1 (TE85-E4-ORF1), this viral protein displayed almost continuous plasma membrane staining along regions of cell-cell contact where PDZ proteins typically accumulate as well as the previously described punctate cytoplasmic staining (Figure 2a) (Weiss *et al.*, 1996). E4-ORF1 was also present discontinuously at regions of cell-cell contact along the plasma membrane and in the cytoplasm of both CREF-E4-ORF1 cells and 20-8 cells, which are derived from an Ad9-induced rat mammary tumor (Figure 2a). In addition, while exhibiting less punctate cytoplasmic staining than untagged E4-ORF1, fusion proteins consisting of GFP linked to the amino-terminus of E4-ORF1 revealed that wt E4-ORF1 and region I/II

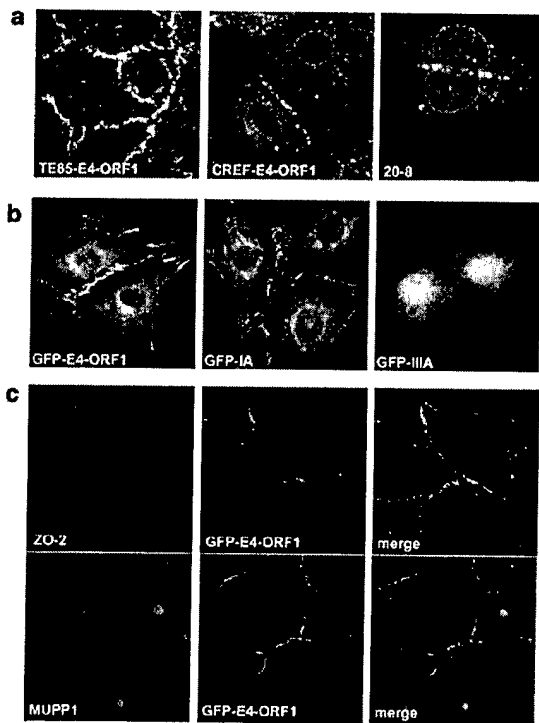


Figure 2 E4-ORF1 and PDZ proteins localize to the plasma membrane. (a) E4-ORF1 localizes to the plasma membrane. TE85-E4-ORF1 cells, CREF-9ORF1-low cells (CREF-E4-ORF1 cells), or 20-8 mammary tumor cells were subjected to indirect IF assays with E4-ORF1 antibodies. In the middle and right panels, cell nuclei are circumscribed by dashed lines to aid visualization of discontinuous E4-ORF1 staining present along the membrane at regions of cell-cell contact. (b) The PDZ domain-binding motif of E4-ORF1 promotes its recruitment to the plasma membrane. CREF cells stably expressing GFP-tagged *wt* or mutant E4-ORF1 proteins were visualized by fluorescence microscopy. Results with GFP-IA or GFP-IIIA are representative of findings with region I/II mutants IIA and IIB or region III mutants T123D and V125A, respectively. (c) E4-ORF1 colocalizes with PDZ proteins at the plasma membrane. TE85 cells stably expressing GFP-tagged *wt* E4-ORF1 were subjected to indirect IF assays with either ZO-2 (top three panels) or MUPP1 (bottom three panels) antibodies and visualized by deconvolution fluorescence microscopy

mutants (IA, IIA, IIB) can localize to the plasma membrane of CREF cells, whereas the GFP moiety alone and region III mutants (IIIA, V125A, T123D) cannot (Figure 2b) (unpublished data). These observations suggest that the PDZ domain-binding motif of E4-ORF1 promotes its recruitment into PDZ-protein complexes at the plasma membrane. Supporting this conclusion, we showed that endogenous ZO-2 and MUPP1 also localize to the plasma membrane at regions of cell-cell contact and, at these sites, display either extensive or partial co-localization, respectively, with GFP-tagged *wt* E4-ORF1 in TE85 (Figure 2c) and CREF cells (unpublished data). The utilization of an optimized paraformaldehyde fixation procedure in these experiments, as opposed to methanol fixation employed previously (Weiss *et al.*, 1997a), substantially improved

our ability to detect E4-ORF1, MUPP1, and ZO-2 at the plasma membrane. These findings are consistent with the notion that E4-ORF1 constitutively stimulates PI3K by binding to and subverting the activity of specific plasma membrane-associated PDZ-protein signaling complexes.

PI3K-dependent activation of PKB by E4-ORF1 in cells

We next investigated whether in cells E4-ORF1 also elevates the activity of the PI3K downstream effector PKB. Our results indicated that transient expression of E4-ORF1 in COS7 cells causes a 10-fold increase in PKB activity (Figure 3a). This effect was stronger than the seven-fold induction in PKB activity produced by the RasV12 oncoprotein (Figure 3a). Additionally, E4-ORF1-mediated PKB stimulation was blocked by wortmannin in COS7 cells (Figure 3a) and, as determined by immunoblot analyses with antibodies that recognize activated PKB, was similarly inhibited in 3T3 cells by treatment with the PI3K inhibitor LY294002 or by overexpression of the p85 PI3K regulatory subunit (Figure 3b), which can act as a dominant negative inhibitor of class I PI3K (Rameh *et al.*, 1995). Therefore, PI3K activation mediated by E4-ORF1 results in potent stimulation of PKB in cells. The observation that RasV12, but not E4-ORF1, could enhance the activity of ERK2 in COS7 cells (Figure 3c) or CREF cells (unpublished data) underscores the selective capacity of E4-ORF1 to activate the PI3K pathway.

The relation between PKB activation and transformation by E4-ORF1 was assessed in CREF cells transiently expressing either *wt* or mutant E4-ORF1 proteins. Utilizing antibodies that recognize activated PKB, we demonstrated that *wt* E4-ORF1 and the control transformation-proficient mutant T108S, but none of the transformation-deficient mutants, are capable of stimulating PKB (Figure 3d). These results are fully concordant with the PI3K-activation phenotypes of these E4-ORF1 proteins (see Figure 1b). Also notable is that E4-ORF1 mutants IIIC and IIID, which have weak transforming activity owing to region III mutations that decrease but do not eliminate the function of the PDZ domain-binding motif (Weiss and Javier, 1997), showed a reduced capacity to activate PKB (Figure 3d). Other results showed that E4-ORF1 proteins encoded by Ad12, Ad3, Ad5, or Ad9, representative human Ads from subgroup A, B, C, or D, respectively, share the ability to stimulate PKB in COS7 cells (Figure 3e) in a PI3K-dependent manner (unpublished data), thereby revealing a common activity for these viral polypeptides.

We also tested whether E4-ORF1 stimulates PKB during a productive *wt* Ad9 infection of human A549 cells. Virus Ad9-IIIA encoding the mutant *E4-ORF1 IIIA* gene, which fails to activate PI3K or PKB in cells (see Figures 1b and 3d), was included as a negative control in the assays. We found that activated PKB was evident at 8 h postinfection with *wt* Ad9 and persisted at 24 h postinfection, but failed to accumulate at any time

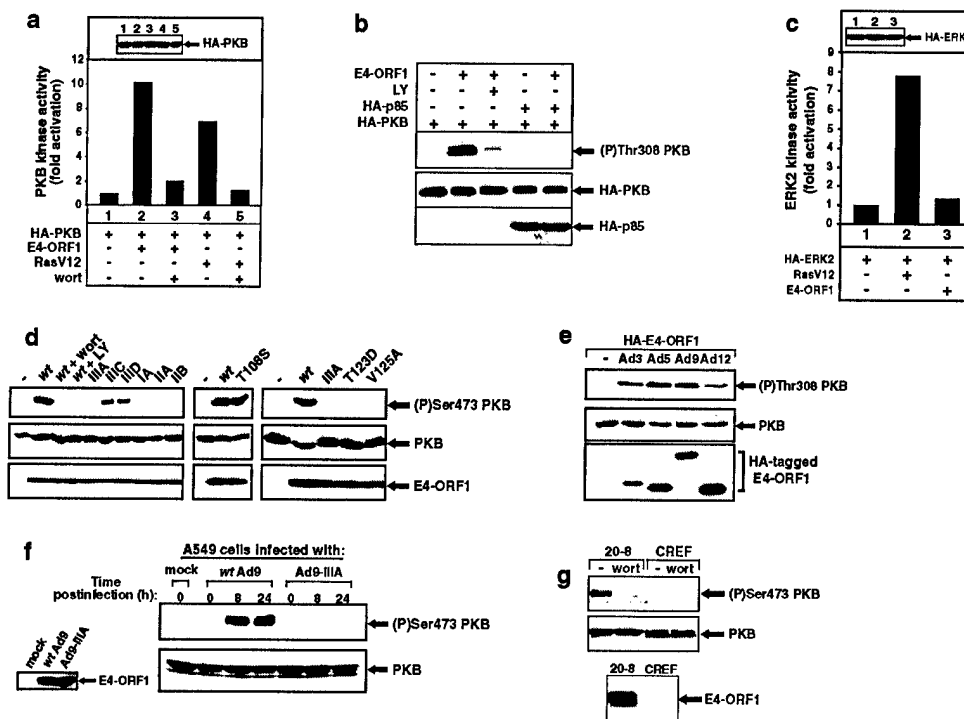


Figure 3 E4-ORF1 selectively activates PKB in a PI3K-dependent manner. **(a)** Stimulation of PKB activity by E4-ORF1. COS7 cells on 10-cm dishes were lipofected with pCDNA3-HA-PKB (1.6 μ g), pGW1 encoding wt E4-ORF1 (6.4 μ g), and pSG5-RasV12 (6.4 μ g). Extracts (200 μ g protein) from serum-starved cells were immunoprecipitated with anti-HA antibodies, and immunocomplexes were subjected to *in vitro* kinase assays with H2B substrate or to immunoblot analyses with anti-HA antibodies (inset panel). Indicated cells were treated with 100 nM wortmannin (wort). One representative experiment is shown. **(b)** Overexpression of p85 inhibits E4-ORF1-mediated PKB activation. NIH 3T3 cells on 6-cm dishes were lipofected with pGW1-HA-PKB (0.5 μ g), pGW1 encoding wt E4-ORF1 (20 ng), and pCG-HA-p85 (2 μ g). Serum-starved cells were lysed in RIPA buffer, and extracts (75 μ g protein) were immunoblotted with anti-(P)Thr308 PKB or anti-HA antibodies. Indicated cells were treated with 50 μ M LY294002 (LY). **(c)** E4-ORF1 fails to activate ERK2 in COS7 cells. COS7 cells on 10-cm dishes were lipofected with pCEP4-HA-ERK2 (1.6 μ g), pGW1 encoding wt E4-ORF1 (6.4 μ g), and pSG5-RasV12 (6.4 μ g). Extracts (200 μ g protein) from serum-starved cells were immunoprecipitated with anti-HA antibodies, and immunocomplexes were subjected to *in vitro* kinase assays with MBP substrate (bottom panel) or to immunoblot analyses with anti-HA antibodies (top panel). One representative experiment is shown. **(d)** Transformation by E4-ORF1 is intimately linked to its ability to activate PKB. CREF cells on 6-cm dishes were lipofected with pGW1 (–) and pGW1 encoding wt or the indicated mutant E4-ORF1 (right and left panels) (2 μ g each) or pCMV_{Bam3}-Neo (–) and pCMV_{Bam3}-Neo encoding wt or mutant T108S E4-ORF1 (center panel) (2 μ g each). Serum-starved cells were lysed in sample buffer, and extracts (100 μ g protein) were immunoblotted with anti-(P)Ser473 PKB, anti-PKB, or anti-E4-ORF1 antibodies. Indicated cells were treated with 100 nM wortmannin (wort) or 50 μ M LY294002 (LY). **(e)** Stimulation of PKB by E4-ORF1 proteins derived from representative subgroup A–D human Ads. COS7 cells on 6-cm dishes were lipofected with pCMV_{Bam3}-Neo (–) and pCMV_{Bam3}-Neo plasmids encoding the indicated HA epitope-tagged E4-ORF1 (1.5 μ g each). Serum-starved cells were lysed in RIPA buffer, and extracts (100 μ g protein) were immunoblotted with anti-(P)Thr308 PKB, anti-PKB, or anti-HA antibodies. **(f)** E4-ORF1 activates PKB in Ad9-infected permissive cells. Serum-starved A549 cells were mock infected or infected at a multiplicity of 10 with wt Ad9 or mutant Ad9-IIIa. At the indicated times postinfection, extracts (75 μ g protein) in sample buffer were immunoblotted with anti-(P)Ser473 PKB, anti-PKB, or anti-E4-ORF1 antibodies. **(g)** Constitutive activation of PKB in an Ad9-induced tumor cell line. Confluent serum-starved 20-8 cells or control CREF cells were lysed in RIPA buffer, and extracts (100 μ g protein) were immunoblotted with anti-(P)Ser473 PKB or anti-PKB antibodies (top panels). CREF and 20-8 extracts were also immunoprecipitated with anti-E4-ORF1 antibodies, and recovered proteins were immunoblotted with the same antibodies (bottom panel). Indicated cells were untreated (–) or treated with 100 nM wortmannin (wort).

post-infection with Ad9-IIIa, despite the fact that both viruses exhibited comparable E4-ORF1 protein expression and replication in A549 cells (Figure 3f) (unpublished data). Furthermore, unlike control CREF cells, 20-8 mammary tumor cells displayed constitutively high levels of activated PKB that was ablated by wortmannin (Figure 3g), suggesting that dysregulated PI3K signaling also contributes to Ad9-induced mammary tumorigenesis.

Abrogation of E4-ORF1-mediated PKB activation by overexpression of PDZ proteins

As our findings with E4-ORF1 mutants indicated that activation of PI3K and PKB by E4-ORF1 depends on its interactions with cellular PDZ proteins, we expected that overexpression of MUPP1, MAGI-1, ZO-2, or DLG would affect the ability of E4-ORF1 to stimulate this signaling cascade. The results showed that over-

expression of each *wt* PDZ protein individually suppresses E4-ORF1-mediated PKB stimulation in 3T3 cells (Figures 4a-d). This effect precisely correlated with the capacities of the PDZ proteins to complex with E4-ORF1 because PDZ-protein deletion mutants able to bind E4-ORF1 (MUPP1-PDZ10-13, MAGI-1- Δ PDZ1, - Δ PDZ2, - Δ PDZ3, - Δ PDZ4, - Δ PDZ5, - Δ PDZ3+4, - Δ PDZ3+5, - Δ PDZ4+5, ZO-2-NT) (Glaunsinger *et al.*, 2000, 2001; Lee *et al.*, 2000) blocked E4-ORF1-mediated PKB activation, whereas deletion mutants unable to bind E4-ORF1 (MUPP1- Δ PDZ7+10, -PDZ11-13, MAGI-1- Δ PDZ1+3, ZO-2- Δ PDZ1, DLG- Δ PDZ1+2) (Glaunsinger *et al.*, 2000, 2001; Lee *et al.*, 1997, 2000) did not (Figures 4a-d). These results provide additional evidence demonstrating that interactions with one or more PDZ-protein targets are crucial for E4-ORF1 to activate PI3K signaling in cells.

PI3K-dependent stimulation of S6K by E4-ORF1

One of the downstream effectors of PKB is the regulator of translation and cell-cycle progression S6K (Cantrell, 2001). In COS7 cells, E4-ORF1 and RasV12 comparably increased the activity of S6K by three-fold (Figure 5a). E4-ORF1-mediated S6K stimulation showed an expected sensitivity to wortmannin, as well as to rapamycin (Figure 5a), a specific inhibitor of the protein kinase mTOR required for activation of S6K (Dufner and Thomas, 1999). Using antibodies that recognize activated S6K (Dufner and Thomas, 1999), we also showed that, compared to control CREF cells, both CREF-E4-ORF1 cells and 20-8 mammary tumor cells have constitutively high levels of activated S6K that could be eliminated by wortmannin or rapamycin (Figure 5b,c). Our inability to detect constitutively

activated S6K in CREF lines stably expressing transformation-deficient mutants IA, IIA, IIB, and IIIA (Figure 5b) further implicated this activity in E4-ORF1-mediated transformation.

Inactivation of FKHL1 and downregulation of p27kip1 in E4-ORF1-expressing cells

Activated PKB phosphorylates and inactivates FKHL1, a Forkhead-family transcription factor that promotes programmed cell death and blocks cell-cycle progression by stimulating expression of proapoptotic factors (Brunet *et al.*, 1999) and the cyclin-dependent kinase inhibitor p27kip1 (Medema *et al.*, 2000), respectively. In 3T3 cells transfected with a luciferase reporter plasmid containing a Forkhead-responsive promoter, we found that expression of *wt* FKHL1 induces an approximately twofold increase in luciferase activity (Figure 6a). Coexpression with E4-ORF1 blocked the activity of *wt* FKHL1 but not constitutively active mutant FKHL1 TM (Figure 6a), which cannot be phosphorylated by PKB (Brunet *et al.*, 1999). The results of immunoblot analyses with antibodies that recognize phosphorylated, inactive FKHL1 (Brunet *et al.*, 1999) showed that, compared to control CREF cells, CREF-E4-ORF1 cells have elevated levels of phosphorylated FKHL1 that were substantially diminished by LY294002 (Figure 6b). Expression of p27kip1 was also downregulated in CREF-E4-ORF1 cells in a PI3K-dependent manner (Figure 6c).

Inhibition of E4-ORF1-induced transformation by LY294002 or rapamycin

Our findings with E4-ORF1 mutants suggested that transformation by *wt* E4-ORF1 depends on its ability to

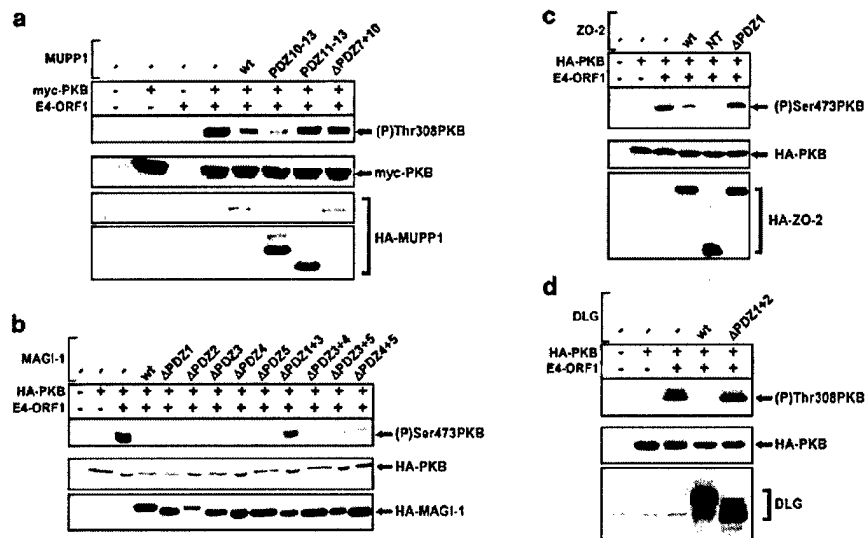


Figure 4 Overexpression of PDZ proteins inhibits E4-ORF1-mediated PKB activation. NIH 3T3 cells on 6-cm dishes were lipofected with pGW1-HA-PKB or pGW1-myc-PKB (0.5 μ g), pGW1 encoding *wt* E4-ORF1 (20 ng), and pGW1 encoding HA epitope-tagged or untagged *wt* or indicated mutant (a) MUPP1 (2.5 μ g), (b) MAGI-1 (0.5 μ g), (c) ZO-2 (0.5 μ g), or (d) DLG (1 μ g). Serum-starved cells were lysed in RIPA buffer, and extracts (60 μ g protein) were immunoblotted with anti-HA, anti-myc, and/or DLG antibodies and also with anti-(P)Thr308 PKB or anti-(P)Ser473 PKB antibodies

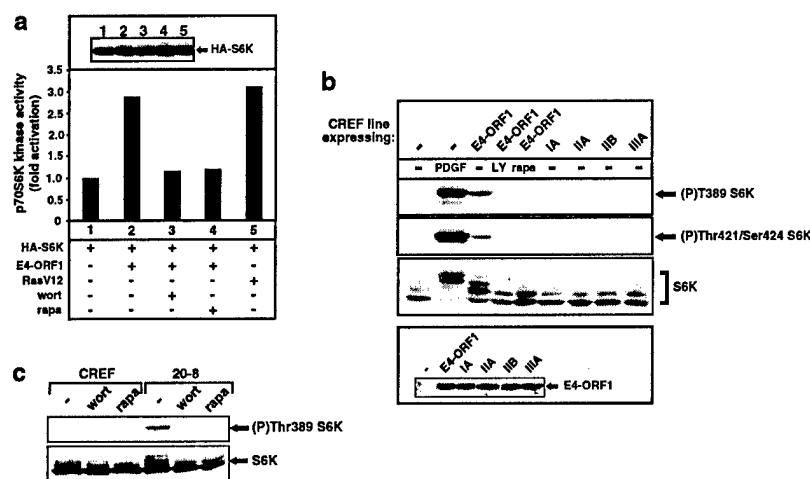


Figure 5 E4-ORF1 activates S6K. (a) Activation of S6K enzymatic activity by E4-ORF1. COS7 cells on 6-cm dishes were lipofected with PMT2-HA-p70 S6K (0.15 μ g), pGW1 encoding wt E4-ORF1 (50 ng), and RasV12 (0.1 μ g). Extracts (200 μ g protein) from serum-starved cells were immunoprecipitated with anti-HA antibodies. Recovered proteins were subjected to *in vitro* kinase assays with an RRRLLSLRA peptide substrate or immunoblotted with anti-HA antibodies (inset panel). Indicated cells were treated with 100 nM wortmannin (wort) or 20 ng/ml rapamycin (rapa). One representative experiment is shown. (b) The transforming potential of E4-ORF1 is linked to its ability to activate S6K. Serum-starved CREF cells stably expressing wt E4-ORF1, the indicated mutant E4-ORF1, or no E4-ORF1 (-) were lysed in RIPA buffer, and extracts (85 μ g protein) were immunoblotted with anti-(P)Thr389 S6K, anti-(P)Thr421/Ser424 S6K, anti-S6K, or anti-E4-ORF1 antibodies. Indicated cells were treated with 20 ng/ml PDGF, 50 μ M LY294002 (LY), or 20 ng/ml rapamycin (rapa). (c) Constitutive activation of S6K in an Ad9-induced mammary tumor cell line. Extracts (100 μ g protein) from 20-8 mammary tumor cells or control CREF cells in RIPA buffer were immunoblotted with anti-(P)Thr389 S6K or anti-S6K antibodies. Indicated cells were untreated (-) or treated with either 100 nM wortmannin (wort) or 20 ng/ml rapamycin (rapa)

activate PI3K in cells. In an attempt to provide direct support for this idea, we tested whether the LY294002 can block transformation by E4-ORF1 in CREF cells. Our results showed that LY294002 greatly diminishes the ability of CREF-E4-ORF1 cells to form colonies in soft agar (Figure 7a), and also causes a 25-fold decrease in E4-ORF1-mediated focus formation on CREF cells (Figure 7b). Rapamycin has been reported to block transformation by constitutively activated forms of PI3K and PKB but not by 11 other oncoproteins (Aoki *et al.*, 2001), so we also examined this drug in our transformation assays. Rapamycin likewise abrogated E4-ORF1-mediated soft-agar growth and focus formation in CREF cells (Figure 7a,b). It is important to note that, whereas the low doses of drugs employed in these assays robustly inhibited both transformed growth properties and activation of PI3K and/or S6K induced by E4-ORF1 in CREF cells, neither the viability nor growth of normal CREF cells was appreciably affected under these conditions (unpublished data). These findings demonstrate that the transforming potential of E4-ORF1 depends on its ability to activate the PI3K pathway in cells.

Association of PI3K activation by E4-ORF1 with Ad9-induced mammary tumorigenesis

In an effort to similarly, directly link PI3K activation by E4-ORF1 to Ad9-induced mammary tumorigenesis, we investigated whether LY294002 and rapamycin can reverse the transformed growth properties of 20-8

mammary tumor cells. Like CREF-E4-ORF1 cells, 20-8 cells grew efficiently in soft agar yet, in the presence of either drug, this growth was substantially reduced (Figure 7c), albeit more efficiently, with LY294002 than with rapamycin. To provide additional evidence relating PI3K activation by E4-ORF1 to Ad9-induced mammary tumorigenesis, we determined the tumorigenic potentials of a collection of E4-ORF1 mutant Ad9 viruses. The results revealed that Ad9 viruses coding for E4-ORF1 mutants unable or having a limited capacity to stimulate the PI3K pathway fail to elicit tumors of any kind in rats (Table 1), despite the fact that such viruses display wt E4-ORF1 protein expression and replication in A549 cells (unpublished data). In contrast, the control Ad9 virus coding for E4-ORF1 mutant T108S, which stimulates the PI3K pathway similar to wt E4-ORF1 (see Figure 3d), behaved like wt Ad9 in generating mammary tumors in 100% of infected female rats (Table 1). Collectively, these findings strongly argue that E4-ORF1-mediated stimulation of PI3K is required for Ad9-induced mammary tumorigenesis in animals.

Discussion

In this paper, we demonstrated that interactions between the Ad9 E4-ORF1 oncoprotein and cellular PDZ proteins result in constitutive stimulation of cellular PI3K, as well as its downstream effectors PKB

a

FKHLR1 reporter	FKHLR1	FKHLR1 TM	E4-ORF1	Relative luciferase activity (fold activation)
+	+	-	-	1.0
+	-	-	-	~1.9
+	+	-	+	~1.1
+	-	+	-	~2.7
+	+	+	+	~2.8

b

c

and S6K (Figures 1, 3, and 5). These findings are significant in uncovering a new PDZ-protein-dependent mechanism for the activation of the PI3K signaling pathway. Consistent with the established link between dysregulation of this signaling pathway and cancer, we also showed that the ability of E4-ORF1 to activate PI3K is required both for E4-ORF1-mediated transformation of cells and for Ad9-induced mammary tumorigenesis in animals (Figure 7 and Table 1). The fact that stimulation of the PI3K cascade engenders a potent survival signal in cells may indicate that E4-ORF1 likewise functions during the Ad life cycle to block programmed cell death.

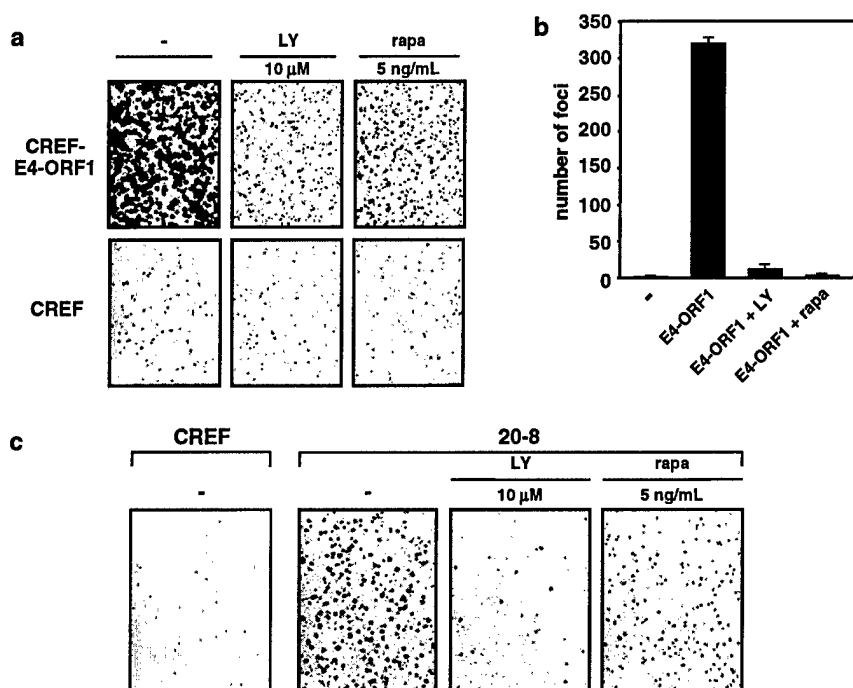


Figure 7 LY294002 or rapamycin blocks transformation by E4-ORF1. (a) Soft-agar growth inhibition of E4-ORF1-expressing CREF cells by LY294002 and rapamycin. An equal number of CREF-E4-ORF1 cells or control CREF cells was suspended in soft agar without (–) or with the indicated amount of LY294002 (LY) or rapamycin (rapa) for 2 weeks and then photographed. (b) Inhibition of E4-ORF1-mediated focus formation by LY294002 and rapamycin. CREF cells on 10-cm dishes were lipofected with pJ4 Ω or pJ4 Ω plasmid encoding *wt* E4-ORF1 (8 μ g each). At 1-week posttransfection, indicated cells were cultured in a medium containing either 10 μ M LY294002 (LY) or 5 ng/ml rapamycin (rapa). Foci were quantified 3–weeks post-transfection. Error bars indicate range of focus numbers obtained on duplicate dishes. (c) Soft-agar growth inhibition of Ad9-induced mammary tumor cells by LY294002 and rapamycin. An equal number of 20-8 mammary tumor cells or control CREF cells was analysed as described above in (a)

Table 1 Mammary tumorigenic phenotypes of *E4-ORF1* mutant Ad9 viruses

Ad9 <i>E4-ORF1</i> gene	Tumorigenic potential in context of Ad9 ^a (No. of rats that developed tumors/rats infected with virus)	
	Females	Males
<i>wt</i>	3/3	0/2
T108S	4/4	0/3
<i>Region I/II mutants</i>		
IA	0/5	0/3
IIA	0/4	0/3
IIB	0/5	0/4
<i>Region III mutants</i>		
IIIA	0/7	0/4
T123D	0/5	0/2
V125A	0/5	0/2
IIIC	0/5	0/3
IIID	0/5	0/4

^aNewborn Wistar–Furth rats were injected subcutaneously with 7×10^7 PFU of virus and monitored by palpation for mammary tumor development for eight months

et al., 2002). Thus, the oncogenic potential of E4-ORF1 may result from its combined capacities to activate PI3K by modifying PDZ-protein complexes at the plasma

membrane and to inhibit antiproliferative signals by sequestering nuclear/cytoplasmic forms of the PDZ proteins.

We do not understand how E4-ORF1 selectively stimulates the PI3K signaling pathway. As PDZ proteins typically link membrane receptors to cytosolic signaling factors, one possibility is that the PDZ-protein targets of E4-ORF1 organize membrane protein complexes that function specifically to modulate signal transduction both to and from PI3K. Selective PI3K stimulation by E4-ORF1 might therefore occur through its ability to disregulate the activity of such specialized complexes. Regarding the possible nature of these protein complexes, PDZ proteins have been associated with monomeric/heterotrimeric G proteins and receptor tyrosine kinases (Lou *et al.*, 2001), which can transduce activation signals to PI3K (Blume-Jensen and Hunter, 2001), and also with the tumor-suppressor protein PTEN, which can antagonize activation signals emanating from PI3K. Interestingly, two recent studies demonstrated that the MAGI-1-related proteins MAGI-2 and MAGI-3 are able to bind PTEN and to increase its ability to repress PI3K signaling (Wu *et al.*, 2000a,b). We have found that MUPP1, MAGI-1, and DLG can likewise form complexes with PTEN (unpublished data). Thus, an intriguing scenario is that potent PDZ-protein-dependent

stimulation of the PI3K signaling pathway by E4-ORF1 involves not only activation of PI3K but also inhibition of PTEN.

Materials and methods

Plasmids

E4-ORF1 genes were introduced into pJ4 Ω (Weiss *et al.*, 1997a), pBABE-puro (Morgenstern and Land, 1990), pGW1 (British Biotechnologies), and pEGFP-C3 (Clontech) expression plasmids. pCMV_{Bam3-Nco} plasmids expressing E4-ORF1 (Weiss *et al.*, 1997a,b) and pGW1 plasmids expressing amino-terminal HA epitope-tagged MAGI-1, MAGI-1 Δ PDZ1, MAGI-1 Δ PDZ3, MAGI-1 Δ PDZ1+3, MAGI-1 Δ SPDZ, ZO-2, ZO-2 Δ PDZ1, MUPP1, or MUPP1 Δ PDZ7+10 (Glaunsinger *et al.*, 2000, 2001; Lee *et al.*, 2000) were described previously. Plasmids were also generously supplied by Julian Downward (pSG5-RasV12, pGFP-AH, pGFP-AH^{R25C}), Melanie Cobb (pCEP4-HA-ERK2), James Woodgett (pCDNA3-HA-PKB), Arnold Levine (pSP72-RasV12), Lewis Williams (pCG-HA-p85), Joseph Avruch (pMT2-HA-p70S6K), Michael Greenberg (pECE-HA-FKHRL1 *wt*, pECE-HA-FKHRL1 TM, pGL3-(3x)FHRE, pEF-lacZ), Kyung-Ok Cho (pGW1-HA-SAP97), and Guy James (pCDNA3-MAGI-1b- Δ PDZ2 (aa 625–702 deleted), Δ PDZ4 (aa 953–1025 deleted), Δ PDZ5 (aa 1043–1116 deleted), Δ PDZ3+4, Δ PDZ3+5, Δ PDZ4+5). After attachment of an HA-epitope tag at their amino-termini, MAGI-1b deletion-mutant cDNAs were introduced into pGW1, as were cDNAs coding for RasV12, MUPP1-PDZ10-13 (aa 1531–2054), MUPP1-PDZ11-3 (aa 1701–2054), SAP97 Δ PDZ1+2 (aa 226–368 deleted), ZO-2-NT (aa 1–572), and amino-terminal myc epitope-tagged PKB.

Cells

Cells were maintained in culture medium (DME supplemented with gentamicin and FBS). CREF and TE85 lines stably expressing *wt* or mutant Ad9 E4-ORF1 were isolated by selection with a puromycin-resistance marker. With the exception of CREF-9ORF1-low cells, which express low levels of the E4-ORF1 protein (Weiss *et al.*, 1997a), pBABE-puro expressing *wt* Ad9 E4-ORF1 was used to establish CREF-E4-ORF1 lines. The 20-8 cell line was derived from an Ad9-induced rat mammary tumor.

Cell transfections and treatments

Transfections were performed according to manufacturers' recommendations using Fugene6 (Roche), Lipofectamine or Lipofectamine plus (Invitrogen Life), or by the calcium phosphate precipitation method (Kingston, 1989). Experimental analyses were routinely conducted 48 h post-transfection. In some experiments, cells were serum starved by incubation in culture medium lacking serum for 16–24 h, at which time, cells were treated for 10–20 min with indicated doses of PDGF-BB (Gibco), wortmannin (Sigma), LY294002 (Cell Signaling Technologies), rapamycin (Sigma), or DMSO vehicle (untreated) as a control.

Antisera and antibodies

Rabbit polyclonal antibodies to Ad9 E4-ORF1, MUPP1, ZO-2, and DLG were described (Javier, 1994; Lee *et al.*, 1997, 2000; Glaunsinger *et al.*, 2001). Antibodies purchased

from Cell Signaling Technologies (anti-Akt, anti-phospho-Akt (Ser473), anti-phospho-Akt(Thr308), anti-S6 Kinase, anti-phospho-S6 Kinase(Thr389), anti-phospho-S6 Kinase(Thr421/Ser424), anti-phospho-FKHRL1(Thr32)), Transduction Labs (anti-p27kip1), Upstate (anti-PI3K p85), Covance (16B12 anti-HA), Santa Cruz (9E10 anti-myc), Southern Biotechnology Associates Inc. (horseradish peroxidase-conjugated goat anti-rabbit and anti-mouse IgG), and Molecular Probes (goat anti-rabbit IgG conjugated to either Alexa Fluor 594 or FITC) were used according to manufacturers' recommendations.

Extract preparation, immunoprecipitations, and immunoblot assays

Methods for preparation of cell extracts in RIPA buffer (50 mM Tris-HCl pH 8.0, 150 mM NaCl, 1% NP-40, 0.5% deoxycholate, 0.1% SDS) or NETN buffer (20 mM Tris-HCl pH 8.0, 100 mM NaCl, 1 mM EDTA, 0.5% NP-40) supplemented with protease inhibitors and phosphatase inhibitors have been described (Lee *et al.*, 1997). Protein concentrations in cell extracts were determined by the Bradford method (Bradford, 1976). Immunoprecipitation and immunoblot analyses were carried out as described previously (Weiss *et al.*, 1996).

In vitro lipid kinase assays

In vitro lipid kinase assays were performed on total cell extracts as described previously (Susa *et al.*, 1992). A Storm Molecular Dynamics Phosphorimager with ImageQuant software was used to quantify the amount of [³²P]-labeled D3-phosphorylated phosphatidylinositol produced in each reaction.

In vitro protein kinase assays

Immunocomplexes of PKB, ERK2, or S6K were subjected to *in vitro* kinase assays with the appropriate protein or peptide substrate by standard methods (Pelech and Krebs, 1987; Coso *et al.*, 1995; Franke *et al.*, 1995). ³²P-labeled protein substrates were separated by SDS-PAGE and quantified with a Storm Molecular Dynamics phosphorimager. ³²P-labeled phosphorylated RRRSSLRA peptide substrate (Upstate Biotech) bound to P81 ion-exchange cellulose (Whatman) was quantified using a Beckman LS 3801 scintillation counter.

Fluorescence microscopy analyses

Immunofluorescence assays were performed as described previously (Weiss *et al.*, 1997a), except that cells grown on coverslips were fixed for 10 min at RT in 4% paraformaldehyde (Polysciences, Inc.) and then permeabilized for 5 min at RT in 0.5% Triton X-100. Coverslips were mounted onto slides with Slowfade Light (Molecular Probes), and cells were visualized with a Zeiss Axioplan 2 epifluorescence microscope and photographed with a CoolSnap HQ CCD camera (Photometrics). Deconvolution microscopy was carried out on a Zeiss Axiovert S100 TV microscope and a Deltavision Restoration Microscopy System. Z-series digital images were deconvolved with the Deltavision constrained iterative algorithm.

Luciferase assays

Cell extracts were subjected to luciferase assays using the Luciferase Assay System (Promega) as recommended by the

manufacturer. Luciferase activities were normalized to β -galactosidase activity generated by pEF-lacZ, which was included as an internal control plasmid in each transfection. β -Galactosidase assays were performed by standard methods (Kingston, 1989).

Focus and soft-agar growth assays

Focus and soft-agar growth assays were carried out as described previously (Javier, 1994; Thomas *et al.*, 1999).

Mutant virus construction, virus infections, and virus tumor assays

Ad9 E4-ORF1 mutant genes were reintroduced into the natural genomic location of an Ad9 infectious plasmid, from which virus was recovered, amplified, and titered as previously described (Thomas *et al.*, 2001). For tumor

studies, newborn Wistar-Furth rats (Harlan Sprague-Dawley, Indianapolis, IN, USA) were subcutaneously inoculated with virus on both flanks (Thomas *et al.*, 2001). Caring and handling of animals were in accordance with the institutional guidelines.

Acknowledgments

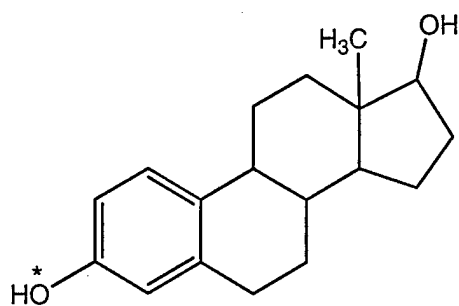
We thank Lyuba Varticovski for suggestions on performing PI3K assays. Predoctoral fellowships from the Viral Oncology Training Grant (T32 CA09197) to KKF and DLT, the US Army Breast Cancer Training Grant (DAMD17-94-J4204) to SSL, RSW, and IJL, and the Molecular Virology Training Grant (T32 AI07471) to BG helped to support this study. This research was funded by grants to RTJ from the National Cancer Institute (RO1 CA58541) and from the US Army (DAMD17-97-1-7082).

References

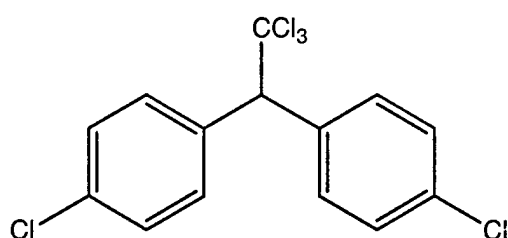
- Aoki M, Blazek E and Vogt PK. (2001). *Proc. Natl. Acad. Sci. USA*, **98**, 136–141.
- Blume-Jensen P and Hunter T. (2001). *Nature*, **411**, 355–365.
- Bowman T, Garcia R, Turkson J and Jove R. (2000). *Oncogene*, **19**, 2474–2488.
- Bradford MM. (1976). *Anal. Biochem.*, **72**, 248–254.
- Brunet A, Bonni A, Zigmond MJ, Lin MZ, Juo P, Hu LS, Anderson MJ, Arden KC, Blenis J and Greenberg ME. (1999). *Cell*, **96**, 857–868.
- Cantrell DA. (2001). *J. Cell Sci.*, **114**, 1439–1445.
- Chang HW, Aoki M, Fruman D, Auger KR, Bellacosa A, Tsichlis PN, Cantley LC, Roberts TM and Vogt PK. (1997). *Science*, **276**, 1848–1850.
- Coso OA, Chiariello M, Yu JC, Teramoto H, Crespo P, Xu N, Miki T and Gutkind JS. (1995). *Cell*, **81**, 1137–1146.
- Dufner A and Thomas G. (1999). *Exp. Cell Res.*, **253**, 100–109.
- Franke TF, Yang SI, Chan TO, Datta K, Kazlauskas A, Morrison DK, Kaplan DR and Tsichlis PN. (1995). *Cell*, **81**, 727–736.
- Glaunsinger BA, Lee SS, Thomas M, Banks L and Javier R. (2000). *Oncogene*, **19**, 5270–5280.
- Glaunsinger BA, Weiss RS, Lee SS and Javier R. (2001). *EMBO J.*, **20**, 5578–5586.
- Gottardi CJ, Arpin M, Fanning AS and Louvard D. (1996). *Proc. Natl. Acad. Sci. USA*, **93**, 10779–10784.
- Hsueh YP, Wang TF, Yang FC and Sheng M. (2000). *Nature*, **404**, 298–302.
- Islas S, Vega J, Ponce L and Gonzalez-Mariscal L. (2002). *Exp. Cell Res.*, **274**, 138–148.
- Javier R, Raska Jr K, Macdonald GJ and Shenk T. (1991). *J. Virol.*, **65**, 3192–3202.
- Javier RT. (1994). *J. Virol.*, **68**, 3917–3924.
- Kimble J and Simpson P. (1997). *Annu. Rev. Cell. Dev. Biol.*, **13**, 333–361.
- Kingston RE. (1989). *Current Protocols in Molecular Biology*. Ausubel FM, Brent R, Kingston RE, Moore DD, Seidman JG, Smith JA, and Struhl K. (eds). Greene Publishing Associates and Wiley-Interscience: New York, NY.
- Kiyono T, Hiraiwa A, Fujita M, Hayashi Y, Akiyama T and Ishibashi M. (1997). *Proc. Natl. Acad. Sci. USA*, **94**, 11612–11616.
- Klippel A, Escobedo MA, Wachowicz MS, Apell G, Brown TW, Giedlin MA, Kavanaugh WM and Williams LT. (1998). *Mol. Cell. Biol.*, **18**, 5699–5711.
- Lee SS, Glaunsinger B, Mantovani F, Banks L and Javier RT. (2000). *J. Virol.*, **74**, 9680–9693.
- Lee SS, Weiss RS and Javier RT. (1997). *Proc. Natl. Acad. Sci. USA*, **94**, 6670–6675.
- Lou X, Yano H, Lee F, Chao MV and Farquhar MG. (2001). *Mol. Biol. Cell.*, **12**, 615–627.
- Medema RH, Kops GJ, Bos JL and Burgering BM. (2000). *Nature*, **404**, 782–787.
- Mills GB, Lu Y, Fang X, Wang H, Eder A, Mao M, Swaby R, Cheng KW, Stokoe D, Siminovich K, Jaffe R and Gray J. (2001). *Semin. Oncol.*, **28**, 125–141.
- Mirza AM, Kohn AD, Roth RA and McMahon M. (2000). *Cell Growth Differ.*, **11**, 279–292.
- Morgenstern JP and Land H. (1990). *Nucleic Acids Res.*, **18**, 3587–3596.
- Muller BM, Kistner U, Veh RW, Cases-Langhoff C, Becker B, Gundelfinger ED and Garner CC. (1995). *J. Neurosci.*, **15**, 2354–2366.
- Nishimura W, Iizuka T, Hirabayashi S, Tanaka N and Hata Y. (2000). *J. Cell Physiol.*, **185**, 358–365.
- Pelech SL and Krebs EG. (1987). *J. Biol. Chem.*, **262**, 11598–11606.
- Rameh LE, Chen CS and Cantley LC. (1995). *Cell*, **83**, 821–830.
- Sheng M and Sala C. (2001). *Annu. Rev. Neurosci.*, **24**, 1–29.
- Susa M, Keeler M and Varticovski L. (1992). *J. Biol. Chem.*, **267**, 22951–22956.
- Suzuki T, Ohsugi Y, Uchida-Toita M, Akiyama T and Yoshida M. (1999). *Oncogene*, **18**, 5967–5972.
- Thomas DL, Schaack J, Vogel H and Javier R. (2001). *J. Virol.*, **75**, 557–568.
- Thomas DL, Shin S, Jiang BH, Vogel H, Ross MA, Kaplitt M, Shenk TE and Javier RT. (1999). *J. Virol.*, **73**, 3071–3079.
- Tsatsanis C and Spandidos DA. (2000). *Int. J. Mol. Med.*, **5**, 583–590.
- Tsunoda S and Zuker CS. (1999). *Cell Calcium*, **26**, 165–171.
- Uthoff SM, Eichenberger MR, McAuliffe TL, Hamilton CJ and Galandiuk S. (2001). *Mol. Carcinogen.*, **31**, 56–62.
- Vogt PK. (2001). *Oncogene*, **20**, 2365–2377.
- Watton SJ and Downward J. (1999). *Curr. Biol.*, **9**, 433–436.
- Weiss RS and Javier RT. (1997). *J. Virol.*, **71**, 7873–7880.

- Weiss RS, Gold MO, Vogel H and Javier RT. (1997a). *J. Virol.*, **71**, 4385–4394.
- Weiss RS, Lee SS, Prasad BV and Javier RT. (1997b). *J. Virol.*, **71**, 1857–1870.
- Weiss RS, McArthur MJ and Javier RT. (1996). *J. Virol.*, **70**, 862–872.
- Woods DF and Bryant PJ. (1991). *Cell*, **66**, 451–464.
- Wu X, Hepner K, Castelino-Prabhu S, Do D, Kaye MB, Yuan XJ, Wood J, Ross C, Sawyers CL and Whang YE. (2000a). *Proc. Natl. Acad. Sci. USA*, **97**, 4233–4238.
- Wu Y, Dowbenko D, Spencer S, Laura R, Lee J, Gu Q and Lasky LA. (2000b). *J. Biol. Chem.*, **275**, 21477–21485.
- Yamada KM and Araki M. (2001). *J. Cell Sci.*, **114**, 2375–2382.
- Yu Y and Sato JD. (1999). *J. Cell. Physiol.*, **178**, 235–246.

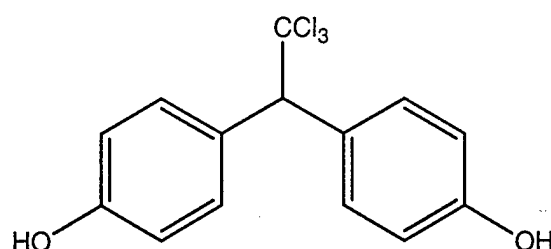
Figure 12



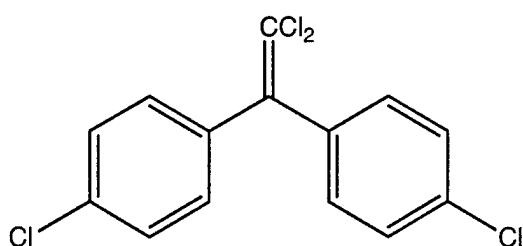
Estradiol (Estrogen)



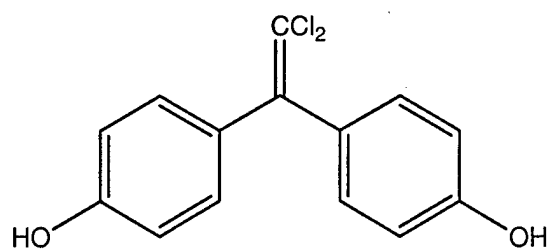
DDT



HPTE



DDE



Dihydroxy-DDE

Structures of Key Compounds. The phenolic OH in estradiol (*) is key for receptor binding and estrogenic activity. Compounds like DDT and DDE have a chlorine in this position whereas hydroxylated metabolites like HPTE and dihydroxy-DDE have the key phenolic group and display both increased estrogen receptor binding and estrogenic activity. See text for details.